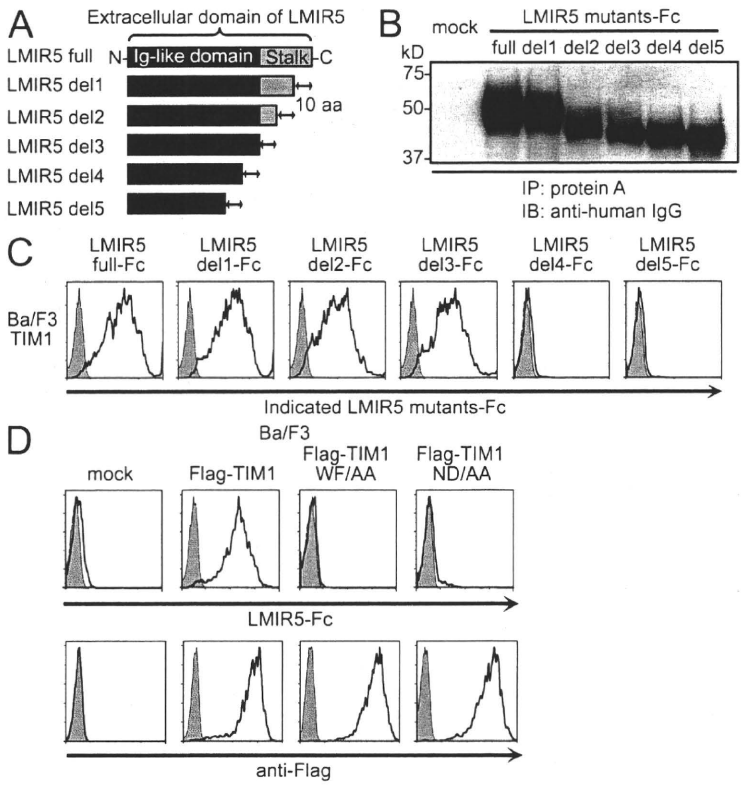

Figure 2. Ig-like domains of both LMIR5 and TIM1 are required for the LMIR5–TIM1 interaction. (A) Structures of LMIR5 extracellular domain in LMIR5-Fc and its deletion mutants. (B) The culture supernatants from 293T cells transduced with LMIR5-Fc or LMIR5-Fc mutants were immunoprecipitated (IP) with protein A, and then immunoblotted (IB) with anti-human IgG antibody. (C) TIM1-transduced Ba/F3 cells were stained with LMIR5-Fc or LMIR5-Fc mutants (continuous line histograms). Control staining with human IgG1 is shown (shaded histograms). (D) Ba/F3 cells transduced with Flag-tagged TIM1, TIM1 (WF/AA), TIM1 (ND/AA), or mock were stained with LMIR5-Fc (top, continuous line histograms) or anti-Flag antibody (bottom, continuous line histograms). Control staining with human (top, shaded histograms) and mouse IgG1 (bottom, shaded histograms) is shown. All data shown are representative of three independent experiments.

domain formed by FG loops of TIM1. Related to this, we found different capabilities of anti-TIM1 antibodies to recognize TIM1 epitopes. Anti-TIM1 antibody (222414) detected TIM1 WT and the ND/AA mutant but not the WF/AA mutant, whereas anti-TIM1 antibody (RMT1-10) detected TIM1 WT and the mutants WF/AA and ND/AA (Fig. S2 A). Thus, anti-TIM1 antibody (222414) presumably recognizes the FG loop structure that is critically maintained by W115/F116 but not N117/D118, whereas anti-TIM1 (RMT1-10) antibody reacts outside this area of TIM1. Then, we compared the inhibitory effect of these antibodies on LMIR5–TIM1 binding. Unlike anti-TIM1 antibody (RMT1-10) or anti-Flag antibody, anti-TIM1 antibody (222414) pretreatment did inhibit LMIR5–TIM1 binding (Fig. S2 B). Collectively, these results suggested that the Ig-like domain of LMIR5 interacted with TIM1 in the region formed by the FG loop of the Ig-like domain, the structure of which was similar or close to the FG–CC' cleft bound by PS, and that it was recognized by anti-TIM1 antibody (222414).

LMIR5 neither binds to PS nor affects TIM1- or TIM4-mediated phagocytosis of apoptotic cells

Given the close proximity of the PS- and LMIR5-binding regions in TIM1, we tested whether LMIR5 interacts with TIM1 through PS. To this end, we performed a protein–lipid overlay assay; although TIM1-Fc bound specifically to PS, as previously reported (Kobayashi et al., 2007; Miyanishi et al., 2007), we found no binding of LMIR5-Fc to PS or to other phospholipids (Fig. 3 A). Consistently, NIH3T3 cells transduced with TIM1 but not LMIR5 promoted phagocytosis of the apoptotic cells through recognition of PS (Fig. 3 B). Next, we asked if the LMIR5–TIM1 interaction affected the TIM1-mediated phagocytosis of the apoptotic cells. As expected, coincubation with anti-TIM1 antibody or TIM1-Fc significantly suppressed phagocytosis of the apoptotic cells in TIM1-expressing NIH3T3 cells (Fig. 3 C). In contrast, coincubation with LMIR5-Fc did not inhibit this phagocytosis (Fig. 3 C). Similarly, the interaction of LMIR5 with TIM4 did not affect TIM4-mediated phagocytosis of the apoptotic cells in peritoneal macrophages (Fig. 3, D and E). Collectively, interaction of neither TIM1 nor TIM4 with LMIR5 affected the phagocytosis of apoptotic cells through its recognition of PS, despite the finding that LMIR5 bound to TIM1 or TIM4 at close proximity to the PS-binding site.

The TIM1–LMIR5 interaction induces LMIR5-mediated activation of mast cells

As previously reported (Kitaura et al., 2003; Yamanishi et al., 2008), LMIR5-mediated activation of mast cells depended on LMIR5 expression levels (Fig. 4 A, left). Notably, stimulation with TIM1-Fc, but not human IgG1 as a control, induced significant levels of extracellular signal-regulated kinase (ERK) activation in LMIR5-transduced BM-derived mast cells (BMMCs), whereas no detectable levels of ERK activation were induced by TIM1-Fc in mock-transduced BMMCs (Fig. 4 A, right). Similarly, stimulation with TIM1-Fc or TIM4-Fc induced cytokine production of fetal liver–derived mast cells (FLMCs) transduced with LMIR5, but not mock-transduced cells (Fig. 4 B; and Fig. S3, A and B). In addition, DAP12 deficiency completely dampened cytokine production of LMIR5-transduced FLMCs stimulated by TIM1-Fc, but not PMA as a control (Fig. 4 B). These results indicated that TIM1-Fc or TIM4-Fc activated mast cells through interaction with LMIR5, which was dependent on the expression levels of LMIR5. As previously reported (Nakae et al., 2007), we found high expression levels of TIM3 as well as

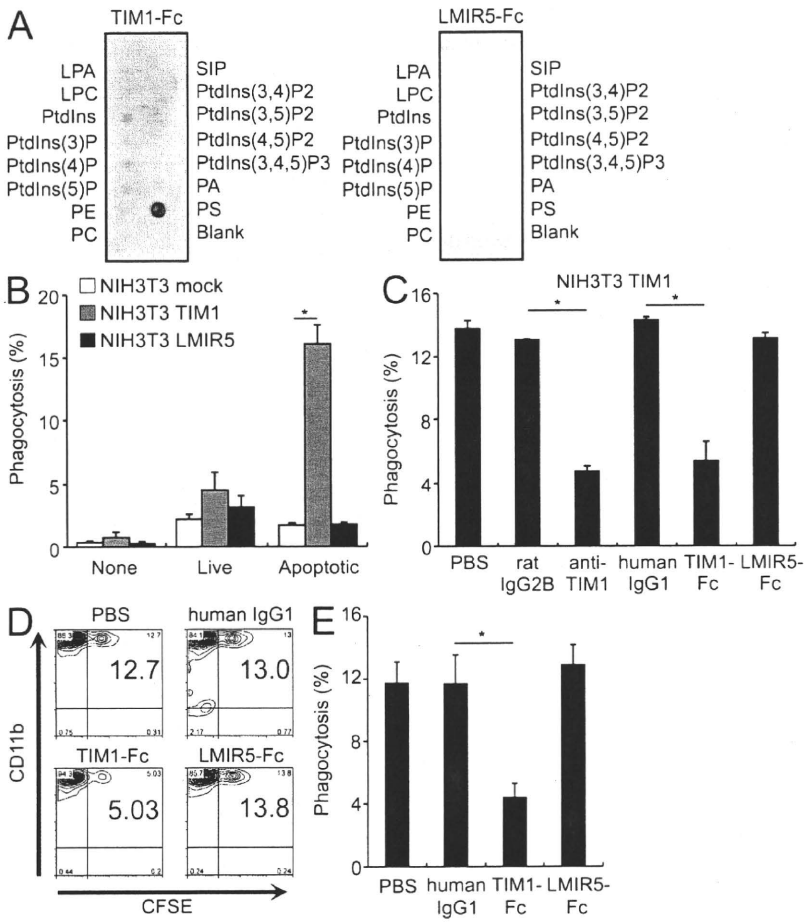

Figure 3. LMIR5 is not involved in TIM1- or TIM4-mediated phagocytosis of apoptotic cells through recognition of PS. (A) PIP strips spotted with the indicated phospholipids were incubated with TIM1-Fc or LMIR5-Fc. (B and C) NIH3T3 cells transduced with either TIM1, LMIR5, or mock were co-cultured with CFSE-labeled live or apoptotic U937 cells in the presence (C) or absence (B) of the indicated antibodies or Fc fusion proteins. The percentage of NIH3T3 cells containing CFSE-labeled U937 cells was determined. (D) Peritoneal macrophages were co-cultured with CFSE-labeled apoptotic thymocytes for 30 min in the presence of 10 µg/ml TIM1-Fc, LMIR5-Fc, or human IgG1. After removal of nonadherent cells, peritoneal macrophages were stained with PE-conjugated anti-CD11b antibody. The percentage of CFSE/CD11b double-positive cells was determined by flow cytometric analysis. (E) Based on the flow cytometric analysis in D, the percentage of phagocytosis is shown. All data points correspond to the means ± SD of triplicate samples. Data are representative of three independent experiments. *, $P < 0.05$.

no detectable expression levels of TIM2 and TIM4 in mast cells (Fig. S4). However, TIM1 expression in mast cells was not confirmed in either protein or transcript levels (Fig. S4). Therefore, we reasoned that the involvement of the TIM1–TIM1/4 interaction in TIM1-Fc–induced activation of mast cells was negligible. We then performed co-culture of LMIR5- or mock-transduced FLMCs with TIM1-transduced Chinese hamster ovary (CHO) cells, demonstrating higher levels of IL-6 released into the supernatants of the former co-culture as compared with the latter (Fig. 4 C, left). In addition, we found higher levels of IL-6 released into the supernatants in the co-culture of LMIR5-expressing FLMCs with TIM1-transduced CHO cells as compared with mock-transduced CHO cells (Fig. 4 C, right). These results indicated that interaction of LMIR5 with surface-expressed TIM1 as well as soluble TIM1 induced the LMIR5-mediated activation of mast cells.

In vivo evidence that the LMIR5–TIM1 interaction induces the accumulation of neutrophils

To investigate the physiological role of TIM1 as a ligand for LMIR5, we generated LMIR5-deficient mice (Fig. S5 A). We confirmed gene targeting by genomic PCR (Fig. S5 B) and the complete absence of LMIR5 expression in BM neutrophils by flow cytometry (Fig. 5 C). Semiquantitative RT-PCR analysis demonstrated no significant difference of LMIR1–4 transcript levels in BM cells between WT and LMIR5$^{-/-}$ mice (Fig. S5 C). LMIR5$^{-/-}$ mice were born at the expected Mendelian ratio and showed no obvious abnormalities. In addition, WT and LMIR5$^{-/-}$ mice did not reveal major differences in the myeloid and lymphoid development of the BM, spleen, thymus, peripheral blood, and peritoneal cells (Fig. S6).

To address the physiological significance of the LMIR5–TIM1 interaction, we chose a model for kidney ischemia/reperfusion injury (IRI; Kelly et al., 1996; Ichimura et al., 1998, 2008; Wu et al., 2007; Lech et al., 2009; Waanders et al., 2010), which is the known in vivo model for TIM1 induction. Consistent with previous reports (Ichimura et al., 1998, 2008; Waanders et al., 2010), TIM1 mRNA levels rapidly increased at day 1 after IRI and diminished through days 2–4 in the IRI kidneys of WT mice, whereas they were maintained at low levels before and after IRI in contralateral kidneys (Fig. 5 A, left). TIM4 mRNA was undetectable in IRI or contralateral kidneys (unpublished data). Notably, LMIR5 mRNA levels increased through days 1 and 2, and thereafter decreased through days 3 and 4 in IRI but not control kidneys of WT mice (Fig. 5 A, right). Further examination showed that in IRI kidneys of WT mice, TIM1 was highly expressed in CD45$^-$ (nonhematopoietic) cells as compared with CD45$^+$ (hematopoietic) cells, whereas LMIR5 was predominantly expressed in CD45$^+$ cells (Fig. 5 B). Together with previous findings (Kelly et al., 1996; Ichimura et al., 1998, 2008; Wu et al., 2007; Lech et al., 2009; Waanders et al., 2010), these results indicated that LMIR5-expressing neutrophils were recruited in IRI kidneys after the up-regulation of TIM1 expression in the renal tubular cells. We then

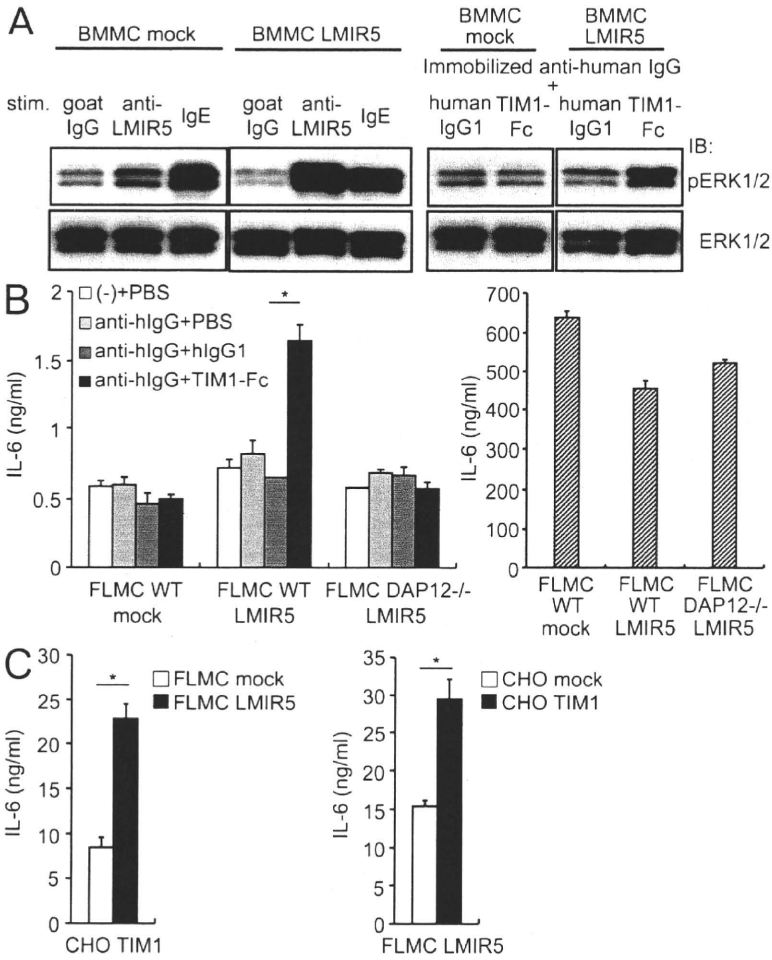

Figure 4. The binding of TIM1 to LMIR5 induced LMIR5-mediated mast cell activation. (A) BMMCs transduced with LMIR5 or mock were stimulated with anti-LMIR5 antibody, goat IgG, or SPE-7 IgE (left), or with TIM1-Fc or human IgG1 (right). Cell lysates were subjected to immunoblotting (IB) with anti-phospho-p44/42 mitogen-activated protein kinase (pERK1/2). One representative out of three independent experiments is shown. (B) Either WT or DAP12-deficient FLMCs transduced with LMIR5 or mock were stimulated with 100 nM PMA (right) or with TIM1-Fc, human IgG1 (hIgG1), or PBS (left). (C) FLMCs transduced with LMIR5 or mock were co-cultured with TIM1-expressing CHO cells (left), or LMIR5-expressing FLMCs were co-cultured with CHO cells transduced with TIM1 or mock for 24 h (right). IL-6 released into the culture supernatants was measured by ELISA. Data are means ± SD of four triplicate samples. One representative out of four independent experiments is shown. Statistically significant differences are shown. *, $P < 0.05$.

compared the IRI kidneys from WT mice with those from LMIR5$^{-/-}$ mice. Flow cytometric analysis delineated that the percentage of neutrophils in IRI kidneys was lower in LMIR5-deficient mice compared with WT mice (Fig. 5 D). On the other hand, in vitro migration assays demonstrated a comparable ability of WT and LMIR5$^{-/-}$ neutrophils to migrate toward chemoattractants such as MIP-2, C5a, KC, and fMLP (Fig. S7 A). To further test if the LMIR5–TIM1 interaction was involved in the neutrophil accumulation in the kidney IRI, we used dorsal air pouch experiments as an in vivo neutrophil recruitment model. Importantly, both TIM1-Fc–induced neutrophil migration and cytokine production in dorsal air pouches were dampened by LMIR5 deficiency, although the response to LPS was comparable between both mice (Fig. 5, E and F). These results suggested that the LMIR5–TIM1 interaction contributed to the accumulation of neutrophils in kidney IRI.

LMIR5 deficiency ameliorates renal tubular damage induced by kidney IRI

Next, we examined if LMIR5 deficiency attenuated the renal damage induced by IRI. As previously reported (Kelly et al., 1996; Wu et al., 2007; Lech et al., 2009), higher amounts of IL-6 and MCP-1 were produced in IRI kidneys compared with contralateral kidneys of WT mice (Fig. 6 A and Fig. S7 B). Notably, LMIR5 deficiency attenuated the increase of cytokine production in IRI kidneys, whereas it did not affect TIM1 expression in IRI kidneys (Fig. 6 A and Fig. S7 B). In WT mice, IL-6 transcripts were equivalently expressed in CD45$^+$ and CD45$^-$ cells of IRI kidneys, whereas MCP-1 transcripts were highly expressed in CD45$^+$ cells (Fig. 6 B). These results indicated a contributory role of CD45$^+$ cells in cytokine/chemokine production of IRI kidneys. Histological analysis of IRI kidneys showed severe tubular damage of WT mice, as indicated by widespread tubular necrosis in the outer medulla and cast formation in the inner medulla at 1 d after IRI (Fig. 6 C). On the other hand, tubular damage was significantly ameliorated by LMIR5 deficiency (Fig. 6 C). Related to this, the number of neutrophils infiltrating the interstitial compartments of IRI kidneys was lower in LMIR5-deficient mice compared with WT mice (Fig. 6, D and E). We found no tubular damage as well as negligible numbers of neutrophils in contralateral kidneys of WT or LMIR5$^{-/-}$ mice (Fig. 6, C and E; and not depicted). Importantly, immunohistological examination displayed the frequent colocalization of LMIR5-expressing neutrophils and TIM1-expressing tubular epithelial cells in IRI kidneys of WT mice (Fig. 6 F). Altogether, LMIR5 deficiency ameliorated ischemia-induced renal tubular damage associated with neutrophil accumulation.

DISCUSSION

Identification of ligands for immune receptors is indispensable for delineation of their biological functions. Recent studies led us to postulate that paired immune receptors have acquired the ability to recognize both endogenous and exogenous ligands (Shiratori et al., 2004; Satoh et al., 2008). The same hypothesis could be applied to LMIR/CD300 family members, but their ligands remained unknown.

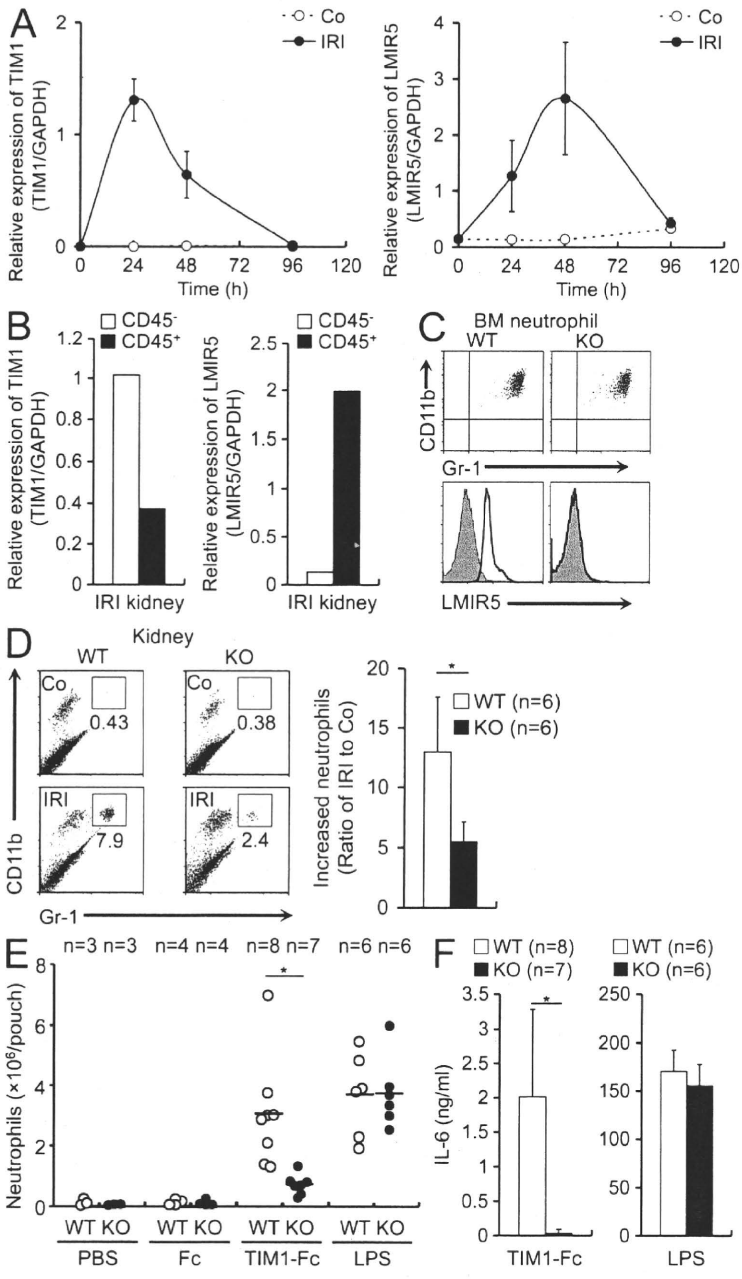

Figure 5. In vivo evidence that the LMIR5–TIM1 interaction induced accumulation of neutrophils. (A and B) Relative gene expression levels of TIM1 (left) or LMIR5 (right) in the IRI or contralateral (Co) kidneys from WT mice at different time intervals after surgery (A) or in the CD45⁻ or CD45⁺ cells sorted from the IRI kidneys of WT mice at 24 h after surgery (B). Data are means ± SD (n = 6 mice in each group). Data are representative of three independent experiments. (C) Surface expression levels of LMIR5 (bottom, continuous line histograms) as well as CD11b and Gr-1 (top) were examined in BM neutrophils from WT or LMIR5$^{-/-}$ (KO) mice. Control staining with goat IgG is shown (shaded histograms). Data are representative of five independent experiments. (D) Percentages of CD11b^{+}Gr-1^{+} neutrophils in either contralateral or IRI kidney cells from WT or KO mice at 24 h after surgery (left). The ratio of neutrophil counts in IRI kidneys to those in contralateral kidneys was determined. Data are means ± SD (n = 6 mice in each group; right). Two independent experiments were performed. (E) Either 100 µg TIM1-Fc or control Fc, or 1 mg LPS was injected into the air pouches of WT or LMIR5$^{-/-}$ mice. At 4 h after injection, neutrophils recruited into the pouches were counted. Each symbol represents an individual mouse. The number of mice in each group is shown. Two independent experiments were performed. (F) IL-6 released into the dorsal air pouches (ELISA). The number of mice in each group is shown. Two independent experiments were performed. Data in D–F are means ± SD. Statistically significant differences are shown. *, $P < 0.05$.

In the present study, we identified TIM1 and TIM4 as endogenous ligands for LMIR5. Because TIM1 and TIM4 play an important role in mediating uptake of apoptotic cells through recognition of PS, we were curious about the specific functions of LMIR5 in a similar context. In fact, the Ig-like domain of LMIR5 bound to TIM1 in the vicinity of the PS-binding site within the Ig-like domain of TIM1 (Fig. 2). However, the LMIR5–TIM1/4 interaction did not hamper the TIM1/4-mediated clearance of apoptotic cells (Fig. 3, C–E). One possible explanation is that TIM1 or TIM4 binds to PS at a higher affinity in comparison to LMIR5. Alternatively, the binding site of TIM1 or TIM4 to LMIR5 might be close, but not identical, to that to PS. In addition, several lines of evidence (Fig. 3, A and B) led us to conclude that LMIR5 is not directly involved in the clearance of apoptotic cells. Because LMIR5 is a DAP12-coupled activating receptor, it is plausible that the LMIR5–TIM1/4 interaction induces activation of LMIR5-expressing mast cells. However, in in vitro experiments, myeloid cells were not activated by the interaction of endogenous LMIR5 and TIM1. As one possible explanation, we assumed that biological events induced by the LMIR5–TIM1 interaction require in vivo environmental factors such as cytokines/chemokines, cell–cell interaction, or cell–extracellular matrix interaction. We also postulated that the biological outcomes induced by the LMIR5–TIM1 interaction might be evident in a pathological situation where soluble TIM1 and/or surface-expressed LMIR5 increase at high levels. To test this, we generated LMIR5-deficient mice and used a mouse model of acute kidney injury, IRI, where TIM1 is up-regulated in the IRI kidney. Intriguingly, LMIR5 deficiency attenuated the acute kidney damage, characterized by tubular necrosis and cast formation. In addition, the recruitment of neutrophils in IRI kidneys, reportedly associated with tissue damage (Kelly et al., 1996; Wu et al., 2007; Bolisetty and Agarwal, 2009; Lech et al., 2009), was suppressed in LMIR5-deficient mice. Notably, IRI induced the marked up-regulation of TIM1 expression in epithelial tubular cells, followed by the recruitment of neutrophils to IRI kidneys. Considering that a large amount of soluble TIM1 is released in the ischemic kidneys, it was possible that LMIR5-expressing myeloid cells interacted with soluble TIM1 or surface TIM1 in

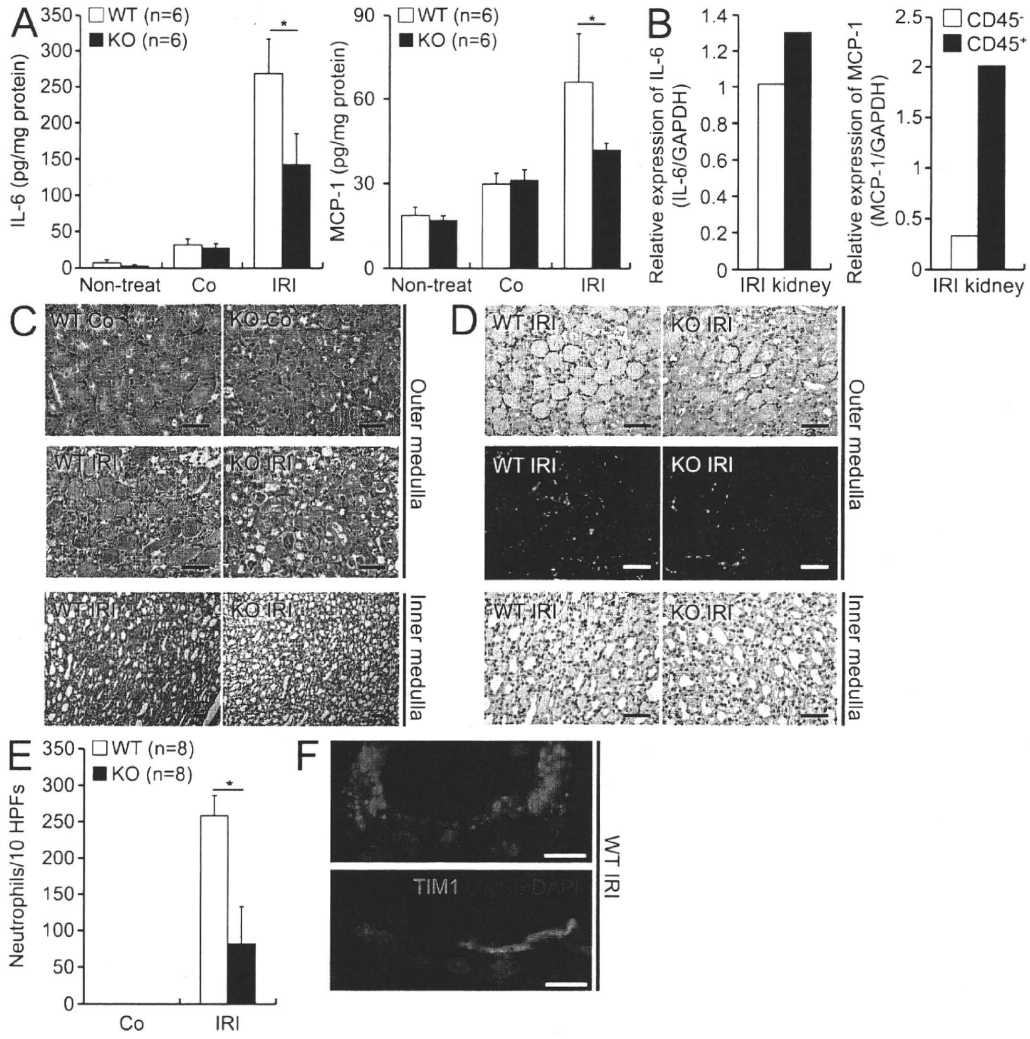

Figure 6. LMIR5$^{-/-}$ mice were protected from renal IRI. (A and B) IL-6 or MCP-1 protein expression (ELISA) in contralateral (Co) or IRI kidneys from WT or LMIR5$^{-/-}$ mice at 24 h after surgery or in nontreated kidneys (A), and relative gene expression levels of IL-6 or MCP-1 (real-time PCR) in CD45^{-} or CD45^{+} cells sorted from IRI kidneys at 24 h after surgery (B). Data are means ± SD (n = 6 mice in each group). Statistically significant differences are shown. *, $P < 0.05$. Data are representative of three independent experiments. (C and D) Tubular injury (C) or neutrophil accumulation within the interstitium in IRI kidneys (D) of WT and LMIR5$^{-/-}$ mice at 24 h after surgery. Representative sections of the outer and inner medulla from contralateral or IRI kidneys from WT and LMIR5$^{-/-}$ mice at 24 h after surgery. (C) Hematoxylin and eosin staining. Bars, 100 µm. Three independent experiments were performed. (D) Immunohistochemical identification of neutrophils (brown) in the outer and inner medulla (top and bottom, respectively). Immunohistochemical identification of neutrophils (green) in the outer medulla (middle). The nuclei were counterstained with DAPI (blue). Bars, 100 µm. Three independent experiments were performed. (E) Neutrophil counts of 10 high-power fields (HPFs) from each section from the outer medulla. Data shown are means ± SD (n = 8 mice in each group). Statistically significant differences are shown. *, $P < 0.05$. Three independent experiments were performed. (F) Immunohistochemical identification of LMIR5-expressing neutrophils (red) and TIM1-expressing epithelial cells (green) in the outer medulla of IRI kidneys of WT mice. The nuclei were counterstained with DAPI (blue). Bars, 10 µm. Three independent experiments were performed. ND, not detected.

epithelial cells. In support of this, histological examination displayed the frequent colocalization of LMIR5-expressing neutrophils and TIM1-expressing epithelial cells in IRI kidneys. Taking these observations together, we assume the relevant mechanism to be as follows. First, soluble TIM1 released from or surface TIM1 expressed by renal tubular cells activates LMIR5-expressing myeloid cells, including resident macrophages/monocytes, mast cells, neutrophils, and dendritic cells through the LMIR5–TIM1 interaction. Then, production of cytokines/chemokines and/or soluble TIM1 promotes the neutrophil recruitment, leading to the renal tubular damage. This scenario was supported by the finding that the neutrophil accumulation induced by TIM1-Fc, a mimic form of soluble TIM1, was dampened by LMIR5 deficiency in the dorsal air pouch experiments. Because the migration of BM neutrophils toward chemoattractants was not affected by LMIR5 deficiency in the in vitro assay (Fig. S7 A), we reasoned that the impaired recruitment of neutrophils in LMIR5-deficient mice was presumably caused by the lack of LMIR5–TIM1 interaction, but not to the

defective migratory function of LMIR5-deficient neutrophils. Of note, neutrophils failed to migrate toward TIM-Fc alone in the in vitro assay (unpublished data), suggesting the requirement of additional signals supplied by the surrounding cells in vivo. We concluded that soluble TIM1 induced the neutrophil accumulation via LMIR5 under in vivo conditions through both direct and indirect mechanisms. However, TIM1-Fc also binds to LMIR5-deficient neutrophils as well as parent Ba/F3 cells (Fig. S1 C and not depicted), suggesting the existence of unidentified ligands for TIM1. Although recent studies implied multiple mechanisms in the pathology of kidney IRI (Kelly et al., 1996; Wu et al., 2007; Bolisetty and Agarwal, 2009; Jang and Rabb, 2009; Lech et al., 2009), the present paper shows that the LMIR5–TIM1 interaction was involved in the tubular damage in the acute phase after IRI.

In conclusion, we provide evidence that TIM1 is a physiological ligand for LMIR5 and that the LMIR5–TIM1 interaction is pivotal in neutrophil accumulation related to tissue damage in kidney IRI. Blocking the LMIR5–TIM1 interaction might be a novel therapeutic strategy for acute renal tubular damage.

MATERIALS AND METHODS

Cells and mice. *DAP12*$^{-/-}$ mice were used as previously described (Kaifu et al., 2003). Animal experiments were conducted in accordance with the guidelines of and with permission provided by the Animal Care and Use Committee of the University of Tokyo (approval no. 20-8). *LMIR5*$^{-/-}$ mice were generated as previously described (Murata et al., 2004). We used *LMIR5*$^{-/-}$ mice that had been backcrossed for at least eight generations with C57BL/6 mice (Charles River).

BM-derived cells, FLMCs, and peritoneal macrophages were generated as previously described (Izawa et al., 2007; Kobayashi et al., 2007; Miyanishi et al., 2007; Yamanishi et al., 2008). Single-cell suspensions of kidney cells were obtained by using Liberase Research Grade Enzyme (Roche).

Antibodies and other reagents. Anti-LMIR5 polyclonal antibody and anti-TIM1 mAb (222414) were obtained from R&D Systems. Biotinylated anti-mouse TIM1 (RMT1-10 or RMT1-4) mAbs were obtained from eBioscience. Anti-mouse TIM1 (RMT1-17), TIM2 (RMT2-14), TIM3 (RMT3-23), and TIM4 (RMT4-54) mAbs have been previously described (Nakayama et al., 2009).

Gene expression analysis. Real-time PCR or RT-PCR was performed using gene-specific primers (Table S1) as previously described (Yamanishi et al., 2008).

Generation of Fc fusion proteins. The cDNA fragments corresponding to the extracellular domains of mouse LMIR1/2/3/4/5, LMIR5 deletion mutants, TIM1, or TIM4 were used. The Fc fusion proteins were purified as previously described (Satoh et al., 2008).

Flow cytometry. In some experiments, cells were stained with 1 μg/ml of Fc fusion proteins or human IgG1 followed by 10 μg/ml of PE-conjugated $F(ab')_2$ donkey anti-human IgG. Flow cytometric analysis was performed with a FACSCalibur (BD) equipped with CellQuest software (BD) and FlowJo software (Tree Star, Inc.), as previously described (Izawa et al., 2007; Yamanishi et al., 2008).

Retrovirus-mediated expression cloning. Expression cloning was performed as previously described (Kitamura et al., 2003). In brief, plasmids (provided by H. Arase, Osaka University, Osaka, Japan) from the cDNA library were transfected into PLAT-E packaging cells (Morita et al., 2000). Infected Ba/F3 cells were stained by LMIR5-Fc. After three rounds of enrichment using a FACSAria (BD), single-cell clones were obtained. The integrated cDNA was recovered by PCR and sequenced.

PIP-strip assay. PIP-strip assay was performed as previously described (Kobayashi et al., 2007). PIP strips were purchased from Echelon Bioscience.

Phagocytosis assay. Phagocytosis assay was performed as previously described (Kobayashi et al., 2007; Miyanishi et al., 2007). CFSE-labeled apoptotic thymocytes were coincubated with peritoneal macrophages in the presence of 10 μg/ml of the Fc fusion proteins indicated in the figures for 30 min. Alternatively, CFSE-labeled live or apoptotic U937 cells were coincubated with NIH3T3 transfectants in the presence of 20 μg/ml of the antibodies or Fc fusion proteins indicated in the figures for 45 min. The percentage of $CSFE^+$ cells was measured by flow cytometric analysis.

Immunoprecipitation and Western blotting. Transfected Ba/F3 cells were incubated with 20 μg/ml LMIR5-Fc, human IgG1, anti-Flag mAb, or mouse IgG1. Cell lysates were immunoprecipitated by using protein A–sepharose. To detect phosphorylation of ERK1/2, transfected BMMCs preincubated with 20 μg/ml TIM1-Fc or human IgG1 for 30 min on ice were stimulated in anti–human IgG antibody–coated plates at 37°C for 7 min, as previously described (Kumagai et al., 2003; Izawa et al., 2007; Yamanishi et al., 2008).

Measurement of cytokines. For co-culture assay, 5×10^4 CHO cells transduced with TIM1 or mock transduced were co-cultured with 2×10^5 FLMCs transduced with LMIR5 or mock transduced for 24 h. Concentrations of IL-6 in the culture supernatants and those of IL-6 and MCP-1 in the renal extract were measured by ELISA, as previously described (Izawa et al., 2007; Wu et al., 2007; Yamanishi et al., 2008). Protein levels of cytokines/chemokines in the renal extract were corrected for the total amounts of protein.

Neutrophil infiltration into mouse dorsal air pouch. Air pouches were formed on the dorsum of mice as previously described (Sin et al., 1986). In brief, 7 ml of sterile air was injected subcutaneously into the back of mice on days 0 and 3. On day 6, 100 μg TIM1-Fc or of control Fc, or 1 mg LPS dissolved in 1 ml of PBS was injected into the air pouches. 4 h after the injection, the air pouches were lavaged. Total cells in the lavage fluid were counted and the percentages of $Gr\text{-}1^+/CD11b^+$ neutrophils were estimated by FACS analysis. IL-6 levels in the lavage fluid were measured by ELISA.

Induction of renal IRI. In brief, the left renal pedicle of male mice was exposed and clamped for 45 min with a microaneurysm clamp via flank incision, as previously described (Lech et al., 2009). Mice were sacrificed at 24, 48, and 96 h after reperfusion. The IRI and contralateral kidneys were collected for histological analysis, flow cytometry analysis, and measurements of cytokines and chemokines.

Histological analysis. Formalin-fixed kidneys were embedded in paraffin and stained with hematoxylin and eosin by standard methods. Neutrophils were detected using rat anti-mouse neutrophil mAb (clone 4/7; AbD Serotec), as previously described (Wu et al., 2007). Neutrophils in the outer medulla were counted in 10 consecutive high-power fields (400×) from each section. Immunofluorescence staining was performed as previously described (Morikawa et al., 2004). In brief, 6-μm-thick frozen sections were stained with primary antibodies: anti-LMIR5 antibody, anti-TIM1 (RMT1-17) mAb, rat anti-mouse neutrophil mAb, and the appropriate secondary antibodies (Jackson ImmunoResearch Laboratories, Inc.). All sections were counterstained with DAPI (Invitrogen).

Statistical analysis. Data are shown as means ± SD. Statistical significance was determined by the Student *t* test, with $P < 0.05$ considered statistically significant.

Online supplemental material. Fig. S1 shows that TIM1 was identified as the ligand for LMIR5 by retrovirus-mediated expression cloning. Fig. S2 shows differential blocking effects of anti-TIM1 antibodies on the TIM1–LMIR5 interaction. Fig. S3 shows that TIM4-Fc as well as TIM1-Fc induced LMIR5-mediated activation of mast cells. Fig. S4 shows no detectable expression levels of TIM1 and TIM4 in BMMCs, FLMCs, or neutrophils. Fig. S5 shows gene targeting of *LMIR5*. Fig. S6 shows normal development of myeloid cells and lymphocytes in LMIR5$^{-/-}$ mice. Fig. S7 shows relative gene expression levels of IL-6, MCP-1, TIM1, or LMIR5 in the postischemic kidneys from WT or LMIR5$^{-/-}$ mice. Table S1 shows the gene-specific primers used in this study. Online supplemental material is available at http://www.jem.org/cgi/content/full/jem.20090581/DC1.

We thank Dr. H. Arase for providing plasmids. We also thank Drs. N. Watanabe and Y. Ishi for cell sorting, and K. Kimura for histological analysis. We are grateful to Dr. D. Wylie for her excellent language support.

This study was supported by grants from the Ministry of Education, Culture, Sports, Science, and Technology (MEXT), Japan, and was in part supported by the Global Center of Excellence Program "Center of Education and Research for the Advanced Genome-Based Medicine-for personalized medicine and the control of worldwide infectious diseases," MEXT, Japan. Y. Yamanishi is supported by a postdoctoral fellowship from the Japan Society for the Promotion of Science.

Dr. T. Kitamura serves as a consultant for R&D Systems. The authors declare no further financial conflicts of interest.

Submitted: 13 March 2009
Accepted: 21 May 2010

REFERENCES

Bailly, V., Z. Zhang, W. Meier, R. Cate, M. Sanicola, and J.V. Bonventre. 2002. Shedding of kidney injury molecule-1, a putative adhesion protein involved in renal regeneration. *J. Biol. Chem.* 277:39739–39748. doi:10.1074/jbc.M200562200

Bolisetty, S., and A. Agarwal. 2009. Neutrophils in acute kidney injury: not neutral any more. *Kidney Int.* 75:674–676. doi:10.1038/ki.2008.689

Chung, D.H., M.B. Humphrey, M.C. Nakamura, D.G. Ginzinger, W.E. Seaman, and M.R. Daws. 2003. CMRF-35-like molecule-1, a novel mouse myeloid receptor, can inhibit osteoclast formation. *J. Immunol.* 171:6541–6548.

Ichimura, T., J.V. Bonventre, V. Bailly, H. Wei, C.A. Hession, R.L. Cate, and M. Sanicola. 1998. Kidney injury molecule-1 (KIM-1), a putative epithelial cell adhesion molecule containing a novel immunoglobulin domain, is up-regulated in renal cells after injury. *J. Biol. Chem.* 273:4135–4142. doi:10.1074/jbc.273.7.4135

Ichimura, T., E.J. Asseldonk, B.D. Humphreys, L. Gunaratnam, J.S. Duffield, and J.V. Bonventre. 2008. Kidney injury molecule-1 is a phosphatidylserine receptor that confers a phagocytic phenotype on epithelial cells. *J. Clin. Invest.* 118:1657–1668.

Izawa, K., J. Kitaura, Y. Yamanishi, T. Matsuoka, T. Oki, F. Shibata, H. Kumagai, H. Nakajima, M. Maeda-Yamamoto, J.P. Hauchins, et al. 2007. Functional analysis of activating receptor LMIR4 as a counterpart of inhibitory receptor LMIR3. *J. Biol. Chem.* 282:17997–18008. doi:10.1074/jbc.M701100200

Jang, H.R., and H. Rabb. 2009. The innate immune response in ischemic acute kidney injury. *Clin. Immunol.* 130:41–50. doi:10.1016/j.clim.2008.08.016

Kaifu, T., J. Nakahara, M. Inui, K. Mishima, T. Momiyama, M. Kaji, A. Sugahara, H. Koito, A. Ujike-Asai, A. Nakamura, et al. 2003. Osteopetrosis and thalamic hypomyelinosis with synaptic degeneration in DAP12-deficient mice. *J. Clin. Invest.* 111:323–332.

Kaplan, G., A. Totsuka, P. Thompson, T. Akatsuka, Y. Moritsugu, and S.M. Feinstone. 1996. Identification of a surface glycoprotein on African green monkey kidney cells as a receptor for hepatitis A virus. *EMBO J.* 15:4282–4296.

Kelly, K.J., W.W. Williams Jr., R.B. Colvin, S.M. Meehan, T.A. Springer, J.C. Gutierrez-Ramos, and J.V. Bonventre. 1996. Intercellular adhesion molecule-1-deficient mice are protected against ischemic renal injury. *J. Clin. Invest.* 97:1056–1063. doi:10.1172/JCI118498

Kitamura, T., Y. Koshino, F. Shibata, T. Oki, H. Nakajima, T. Nosaka, and H. Kumagai. 2003. Retrovirus-mediated gene transfer and expression cloning: powerful tools in functional genomics. *Exp. Hematol.* 31:1007–1014.

Kitaura, J., J. Song, M. Tsai, K. Asai, M. Maeda-Yamamoto, A. Mocsai, Y. Kawakami, F.T. Liu, C.A. Lowell, B.G. Barisas, et al. 2003. Evidence that IgE molecules mediate a spectrum of effects on mast cell survival and activation via aggregation of the FcepsilonRI. *Proc. Natl. Acad. Sci. USA.* 100:12911–12916. doi:10.1073/pnas.1735525100

Klesney-Tait, J., I.R. Turnbull, and M. Colonna. 2006. The TREM receptor family and signal integration. *Nat. Immunol.* 7:1266–1273. doi:10.1038/ni1411

Kobayashi, N., P. Karisola, V. Peña-Cruz, D.M. Dorfman, M. Jinushi, S.E. Umetsu, M.J. Butte, H. Nagumo, I. Chernova, B. Zhu, et al. 2007. TIM-1 and TIM-4 glycoproteins bind phosphatidylserine and mediate uptake of apoptotic cells. *Immunity.* 27:927–940. doi:10.1016/j.immuni.2007.11.011

Kuchroo, V.K., D.T. Umetsu, R.H. DeKruyff, and G.J. Freeman. 2003. The TIM gene family: emerging roles in immunity and disease. *Nat. Rev. Immunol.* 3:454–462. doi:10.1038/nri1111

Kuchroo, V.K., V. Dardalhon, S. Xiao, and A.C. Anderson. 2008. New roles for TIM family members in immune regulation. *Nat. Rev. Immunol.* 8:577–580. doi:10.1038/nri2366

Kumagai, H., T. Oki, K. Tamitsu, S.Z. Feng, M. Ono, H. Nakajima, Y.C. Bao, Y. Kawakami, K. Nagayoshi, N.G. Copeland, et al. 2003. Identification and characterization of a new pair of immunoglobulin-like receptors LMIR1 and 2 derived from murine bone marrow-derived mast cells. *Biochem. Biophys. Res. Commun.* 307:719–729. doi:10.1016/S0006-291X(03)01245-2

Lanier, L.L. 2009. DAP10- and DAP12-associated receptors in innate immunity. *Immunol. Rev.* 227:150–160. doi:10.1111/j.1600-065X.2008.00720.x

Lech, M., A. Avila-Ferrufino, R. Allam, S. Segerer, A. Khandoga, F. Krombach, C. Garlanda, A. Mantovani, and H.J. Anders. 2009. Resident dendritic cells prevent postischemic acute renal failure by help of single Ig IL-1 receptor-related protein. *J. Immunol.* 183:4109–4118. doi:10.4049/jimmunol.0900118

Luo, K., W. Zhang, L. Sui, N. Li, M. Zhang, X. Ma, L. Zhang, and X. Cao. 2001. DIgR1, a novel membrane receptor of the immunoglobulin gene superfamily, is preferentially expressed by antigen-presenting cells. *Biochem. Biophys. Res. Commun.* 287:35–41. doi:10.1006/bbrc.2001.5539

McIntire, J.J., S.E. Umetsu, O. Akbari, M. Potter, V.K. Kuchroo, G.S. Barsh, G.J. Freeman, D.T. Umetsu, and R.H. DeKruyff. 2001. Identification of Tapr (an airway hyperreactivity regulatory locus) and the linked Tim gene family. *Nat. Immunol.* 2:1109–1116. doi:10.1038/ni739

Meyers, J.H., S. Chakravarti, D. Schlesinger, Z. Illes, H. Waldner, S.E. Umetsu, J. Kenny, X.X. Zheng, D.T. Umetsu, R.H. DeKruyff, et al. 2005. TIM-4 is the ligand for TIM-1, and the TIM-1–TIM-4 interaction regulates T cell proliferation. *Nat. Immunol.* 6:455–464. doi:10.1038/ni1185

Miyanishi, M., K. Tada, M. Koike, Y. Uchiyama, T. Kitamura, and S. Nagata. 2007. Identification of Tim4 as a phosphatidylserine receptor. *Nature.* 450:435–439. doi:10.1038/nature06307

Morikawa, Y., S. Tamura, K. Minehata, P.J. Donovan, A. Miyajima, and E. Senba. 2004. Essential function of oncostatin m in nociceptive neurons of dorsal root ganglia. *J. Neurosci.* 24:1941–1947. doi:10.1523/JNEUROSCI.4975-03.2004

Morita, S.T.K., T. Kojima, and T. Kitamura. 2000. Plat-E: an efficient and stable system for transient packaging of retroviruses. *Gene Ther.* 7:1063–1066. doi:10.1038/sj.gt.3301206

Murata, T., K. Furushima, M. Hirano, H. Kiyonari, M. Nakamura, Y. Suda, and S. Aizawa. 2004. ang is a novel gene expressed in early neuroectoderm, but its null mutant exhibits no obvious phenotype. *Gene Expr. Patterns.* 5:171–178. doi:10.1016/j.modgep.2004.08.007

Nakae, S., M. Iikura, H. Suto, H. Akiba, D.T. Umetsu, R.H. Dekruyff, H. Saito, and S.J. Galli. 2007. TIM-1 and TIM-3 enhancement of Th2 cytokine production by mast cells. *Blood.* 110:2565–2568. doi:10.1182/blood-2006-11-058800

Nakayama, M., H. Akiba, K. Takeda, Y. Kojima, M. Hashiguchi, M. Azuma, H. Yagita, and K. Okumura. 2009. Tim-3 mediates phagocytosis

of apoptotic cells and cross-presentation. *Blood.* 113:3821–3830. doi:10.1182/blood-2008-10-185884

Ravetch, J.V., and L.L. Lanier. 2000. Immune inhibitory receptors. *Science.* 290:84–89. doi:10.1126/science.290.5489.84

Santiago, C., A. Ballesteros, L. Martínez-Muñoz, M. Mellado, G.G. Kaplan, G.J. Freeman, and J.M. Casasnovas. 2007a. Structures of T cell immunoglobulin mucin protein 4 show a metal-Ion-dependent ligand binding site where phosphatidylserine binds. *Immunity.* 27:941–951. doi:10.1016/j.immuni.2007.11.008

Santiago, C., A. Ballesteros, C. Tami, L. Martínez-Muñoz, G.G. Kaplan, and J.M. Casasnovas. 2007b. Structures of T cell immunoglobulin mucin receptors 1 and 2 reveal mechanisms for regulation of immune responses by the TIM receptor family. *Immunity.* 26:299–310. doi:10.1016/j.immuni.2007.01.014

Satoh, T., J. Arii, T. Suenaga, J. Wang, A. Kogure, J. Uehori, N. Arase, I. Shiratori, S. Tanaka, Y. Kawaguchi, et al. 2008. PILRalpha is a herpes simplex virus-1 entry coreceptor that associates with glycoprotein B. *Cell.* 132:935–944. doi:10.1016/j.cell.2008.01.043

Shiratori, I., K. Ogasawara, T. Saito, L.L. Lanier, and H. Arase. 2004. Activation of natural killer cells and dendritic cells upon recognition of a novel CD99-like ligand by paired immunoglobulin-like type 2 receptor. *J. Exp. Med.* 199:525–533. doi:10.1084/jem.20031885

Sin, Y.M., A.D. Sedgwick, E.P. Chea, and D.A. Willoughby. 1986. Mast cells in newly formed lining tissue during acute inflammation: a six day air pouch model in the mouse. *Ann. Rheum. Dis.* 45:873–877. doi:10.1136/ard.45.10.873

Umetsu, S.E., W.L. Lee, J.J. McIntire, L. Downey, B. Sanjanwala, O. Akbari, G.J. Berry, H. Nagumo, G.J. Freeman, D.T. Umetsu, and R.H. DeKruyff. 2005. TIM-1 induces T cell activation and inhibits the development of peripheral tolerance. *Nat. Immunol.* 6:447–454. doi:10.1038/ni1186

Waanders, F., M.M. van Timmeren, C.A. Stegeman, S.J. Bakker, and H. van Goor. 2010. Kidney injury molecule-1 in renal disease. *J. Pathol.* 220:7–16. doi:10.1002/path.2642

Wu, H., G. Chen, K.R. Wyburn, J. Yin, P. Bertolino, J.M. Eris, S.I. Alexander, A.F. Sharland, and S.J. Chadban. 2007. TLR4 activation mediates kidney ischemia/reperfusion injury. *J. Clin. Invest.* 117:2847–2859. doi:10.1172/JCI31008

Yamanishi, Y., J. Kitaura, K. Izawa, T. Matsuoka, T. Oki, Y. Lu, F. Shibata, S. Yamazaki, H. Kumagai, H. Nakajima, et al. 2008. Analysis of mouse LMIR5/CLM-7 as an activating receptor: differential regulation of LMIR5/CLM-7 in mouse versus human cells. *Blood.* 111:688–698. doi:10.1182/blood-2007-04-085787

Yotsumoto, K., Y. Okoshi, K. Shibuya, S. Yamazaki, S. Tahara-Hanaoka, S. Honda, M. Osawa, A. Kuroiwa, Y. Matsuda, D.G. Tenen, et al. 2003. Paired activating and inhibitory immunoglobulin-like receptors, MAIR-I and MAIR-II, regulate mast cell and macrophage activation. *J. Exp. Med.* 198:223–233. doi:10.1084/jem.20021825

THE JOURNAL OF BIOLOGICAL CHEMISTRY VOL. 285, NO. 46, pp. 35274–35283, November 12, 2010

Characterization of Leukocyte Mono-immunoglobulin-like Receptor 7 (LMIR7)/CLM-3 as an Activating Receptor

*ITS SIMILARITIES TO AND DIFFERENCES FROM LMIR4/CLM-5**

Received for publication, April 26, 2010, and in revised form, July 30, 2010 Published, JBC Papers in Press, September 3, 2010, DOI 10.1074/jbc.M110.137166

Yutaka Enomoto[‡], Yoshinori Yamanishi[‡], Kumi Izawa[‡], Ayako Kaitani[‡], Mariko Takahashi[‡], Akie Maehara[‡], Toshihiko Oki[‡§], Reiko Takamatsu[¶], Masunori Kajikawa[¶], Toshiyuki Takai[‖], Toshio Kitamura[‡§1], and Jiro Kitaura[‡2]

From the [‡]Division of Cellular Therapy, Advanced Clinical Research Center, Institute of Medical Science, and the [§]Division of Stem Cell Signaling, Center for Stem Cell Therapy, Institute of Medical Science, The University of Tokyo, 4-6-1 Shirokanedai, Minato-ku, Tokyo 108-8639, Japan, [¶]ACTGen Inc., 15-502 Akaho, Komagane-shi, Nagano-ken 399-4117, Japan, and the [‖]Department of Experimental Immunology, Institute of Development, Aging, and Cancer, Tohoku University, 4-1 Seiryo, Sendai 980-8575, Japan

Here we characterize leukocyte mono-Ig-like receptor 7 (LMIR7)/CLM-3 and compare it with an activating receptor, LMIR4/CLM-5, that is a counterpart of an inhibitory receptor LMIR3/CLM-1. LMIR7 shares high homology with LMIR4 in the amino acid sequences of its Ig-like and transmembrane domains. Flow cytometric analysis demonstrated that LMIR4 was predominantly expressed in neutrophils, whereas LMIR7 was highly expressed in mast cells and monocytes/macrophages. Importantly, LMIR7 engagement induced cytokine production in bone marrow-derived mast cells (BMMCs). Although FcRγ deficiency did not affect surface expression levels of LMIR7, it abolished LMIR7-mediated activation of BMMCs. Consistently we found significant interaction of LMIR7-FcRγ, albeit with lower affinity compared with that of LMIR4-FcRγ. Our results showed that LMIR7 transmits an activating signal through interaction with FcRγ. In addition, like LMIR4, LMIR7 synergizes with TLR4 in signaling. Analysis of several chimera receptors composed of LMIR4 and LMIR7 revealed these findings: 1) the transmembrane of LMIR7 with no charged residues maintained its surface expression at high levels in the absence of FcRγ; 2) the extracellular juxtamembrane region of LMIR7 had a negative effect on its surface expression levels; and 3) the strong interaction of LMIR4 with FcRγ depended on the extracellular juxtamembrane region as well as the transmembrane domain of LMIR4. Thus, LMIR7 shares similarities with LMIR4, although they are differentially regulated in their distribution, expression, and function.

A new family of paired immunoreceptors has been recently identified and named leukocyte mono-Ig-like receptor (LMIR)[3]/CMRF-35-like molecules (CLM)/myeloid-associated Ig-like receptor (MAIR)/dendritic cell-derived Ig-like receptor (DIgR)/immune receptor expressed by myeloid cell (IREM)/CD300 (1–15). In mice, there exist at least eight members of the LMIR family (1–9). We and others have previously characterized LMIR1–5 (1–8). An inhibitory receptor, LMIR3/CLM-1, pairs with an activating receptor, LMIR4/CLM-5 or LMIR5/CLM-7. LMIR3 is 91 and 53% identical with LMIR4 and LMIR5, respectively, in the amino acid sequence of the Ig-like domain. In addition, LMIR4 and LMIR5 transmits an activating signal through interaction with FcRγ and DAP12, respectively (2, 3). Consistently, LMIR5 has a positively charged residue (lysine) in the transmembrane domain, which is characteristic of activating receptors interacting with adaptors containing ITAM (3). However, LMIR4 does not have a positively charged residue in the transmembrane domain; instead, it has a negatively charged residue (glutamic acid) (2, 8). Interestingly, the inhibitory receptor LMIR3 also has the potential to transmit an activating signal through interaction with FcRγ in mast cells, despite having no charged residue in the transmembrane domain (4).

FcRγ is an ITAM-bearing signal transduction subunit expressed in a variety of hematopoietic cells (15–19). It is an essential component of the high affinity receptor for IgE (FcεRI) (17), the high affinity IgG receptor (FcγRI) (18), the low affinity IgG receptor (FcγRIII) (19), and the IgA receptor (FcαRI) (20, 21). In addition, FcRγ interacts with various activating receptors such as paired Ig-like receptor A (PIR-A) (22) or platelet collagen receptor glycoprotein VI (23). Although the Arg/Asp charge interaction between transmembrane domains is well characterized, recent studies have also implicated a transmembrane leucine zipper-like interaction between activating receptors and FcRγ (24, 25). However, the relevant molecular mechanism remains incompletely understood.

In the present study, we have characterized LMIR7/CLM-3, which had not been fully analyzed. Structurally, LMIR7 is similar to LMIR4 in its Ig-like and transmembrane domains. The generation of an antibody specifically reacting with LMIR7 enabled us to delineate the differential expression profiles of

* This work was supported by the Ministry of Education, Science, Technology, Sports, and Culture and the Ministry of Health and Welfare, Japan.

[1] To whom correspondence may be addressed: Division of Cellular Therapy, Advanced Clinical Research Center, Inst. of Medical Science, University of Tokyo, 4-6-1 Shirokanedai, Minato-ku, Tokyo 108-8639, Japan. Tel.: 81-3-5449-5759; Fax: 81-3-5449-5428; E-mail: kitamura@ims.u-tokyo.ac.jp.

[2] To whom correspondence may be addressed: Division of Cellular Therapy, Advanced Clinical Research Center, Inst. of Medical Science, University of Tokyo, 4-6-1 Shirokanedai, Minato-ku, Tokyo 108-8639, Japan. Tel.: 81-3-5449-5759; Fax: 81-3-5449-5428; E-mail: kitaura-tky@umin.ac.jp.

[3] The abbreviations used are: LMIR, leukocyte mono-immunoglobulin-like receptor; CLM, CMRF-35-like molecule; BM, bone marrow; PB, peripheral blood; FLMC, fetal liver-derived mast cell; BMMC, bone marrow-derived mast cell; BMMΦ, bone marrow-derived macrophage; BMmDC, bone marrow-derived myeloid dendritic cell; BMpDC, bone marrow-derived plasmacytoid dendritic cell; SCF, stem cell factor; ITAM, immunoreceptor tyrosine-based activation motif; Ab, antibody; PE, phycoerythrin.

LMIR7 and LMIR4. Importantly, LMIR7 engagement led to the activation of bone marrow-derived mast cells (BMMCs) through interaction with FcRγ, validating an activating function of LMIR7 similar to that of LMIR4. Notably, analysis of chimera receptors composed of LMIR4 and LMIR7 revealed that a short extracellular juxtamembrane region of LMIR4 played an important role in its strong interaction with FcRγ. This finding will likely lead us to uncover novel regulatory mechanisms in the interaction of a diverse array of activating receptors with FcRγ.

EXPERIMENTAL PROCEDURES

Antibodies and Other Reagents—Rat anti-LMIR7 IgG_1 monoclonal Ab (mAb) was generated by ACTGen Inc. Anti-FLAG mAb (M2), fluorescein isothiocyanate (FITC)-conjugated anti-FLAG mAb (M2), rabbit anti-FLAG Ab, mouse IgG_1 mAb (MOPC21), and mouse anti-dinitrophenyl (DNP) IgE mAb (SPE-7) were purchased from Sigma-Aldrich. Mouse anti-Myc mAb (9E10) was from Roche Diagnostics. PE- or FITC-conjugated anti-c-Kit, FcεRIα, CD3, B220, NK1.1, F4/80, CD11b, CD11c, or Gr-1 mAbs, Rat IgG_1 mAb, and PE-conjugated streptavidin were from eBioscience. PE-conjugated anti-mouse IgG goat $F(ab')_2$ Ab was from Beckman Coulter. Anti-ERK Ab was from Santa Cruz Biotechnology. Rabbit anti-FcεRI-γ subunit Ab was purchased from Upstate Biotechnology. All of the phospho-specific Abs was purchased from Cell Signaling Technology. Cytokines were obtained from R&D Systems. All other reagents were from Sigma-Aldrich unless stated otherwise.

Cell Culture and Isolation—Murine hematopoietic cell lines and 293T cells were cultured as described (2, 3). C57BL/6 mice (Charles River Laboratories Japan Inc.) were used at 8–10 weeks of age for isolation of tissues and cells such as BM cells, peripheral blood (PB) cells, peritoneal cells, splenocytes, and thymocytes as described (2, 3). All procedures were approved by an institutional review committee. To generate BMMC or fetal liver-derived mast cells (FLMC) with 90% purity (c-Kit^+/$FcεRI^+$ by flow cytometry), BMMCs or FLMCs were cultured in the presence of 10 ng/ml IL-3 alone or with 20 ng/ml stem cell factor (SCF) as described (2–4, 26–29). To generate BM-derived macrophages (BMMΦ), BM-derived myeloid dendritic cells (BMmDC), and BM-derived plasmacytoid dendritic cells (BMpDC), BM cells were cultured in the presence of 10 ng/ml M-CSF, 20 ng/ml GM-CSF, and 50 ng/ml Flt3-ligand, respectively, as described (2–4). BMmDC or BMpDC were sorted by using FITC-conjugated anti-CD11c Ab. BM granulocytes were prepared as described (3). The following mutant mice were used: *FcRγ*$^{-/-}$ (16), *DAP10*$^{-/-}$ (30), and *DAP12*$^{-/-}$ (31).

Gene Expression Analysis—Expression of LMIR7 was analyzed by reverse transcriptase-polymerase chain reaction (RT-PCR) as described (2, 3). Total RNAs were extracted from each cell line and BM-derived cells with TRIzol reagents (Invitrogen), treated with deoxyribonuclease I (Invitrogen), and reverse-transcribed by using High Capacity cDNA Reverse Transcription Kits (Applied Biosystems). A fragment of LMIR7 was amplified with primers 5′-acacccacaacaccaaccac-3′ and 5′-ctgggaagtgtttctctccg-3′. For normalization, a fragment of β-actin was amplified with 5′-catcactattggcaacgagc-3′ and 5′-acgcagctcagtaacagtcc-3′. Relative expression levels of LMIR7 among samples were measured by real-time RT-PCR as described (3). cDNA was amplified using a LightCycler FastStart DNA Master SYBR Green I Kit (Roche Diagnostics) under the following conditions: one cycle of 95 °C for 10 s, 40 cycles of 95 °C for 5 s, and 60 °C for 25 s. All samples were independently analyzed three times. The following primers were used: 5′-acacccacaacaccaaccac-3′ and 5′-accacaaagaccatcagcaaga-3′ for LMIR7; and 5′-atgtgtccgtcgtggatctga-3′ and 5′-ttgaagtcgcaggagacaacct-3′ for GAPDH. Relative gene expression levels were calculated using standard curves generated by serial dilution of cDNA and normalized by a GAPDH expression level. Product quality was checked by melting curve analysis via LightCycler software (Roche Diagnostics).

Plasmid Constructs—We searched the GenBank™/European Molecular Biology Laboratory (EMBL)/DNA Data Bank of Japan (DDBJ) database by using the amino acid sequence of the Ig-like domain of mLMIR1. On the basis of the sequence data, the cDNA of mouse LMIR7 was isolated by PCR with the primers 5′-caccaaggacaggagaggag-3′ and 5′-agggagagggagagggaga-3′ from a cDNA library of BMMCs derived from C57BL/6 mice and its sequence was confirmed (LMIR7/CLM-3: GenBank™ accession number AY457049) (1–3). A cDNA fragment of LMIR7 lacking the signal sequence was tagged with a FLAG or Myc epitope at the N terminus. A SLAM (signaling lymphocyte-activating molecule) signal sequence (32) (a gift from Hisashi Arase, Osaka University, Osaka, Japan), FLAG- or Myc-LMIR7, was subcloned into a pMXs-IRES-puro^r (pMXs-IP) (33) retroviral vector to generate pMXs-FLAG- or Myc-LMIR7-IP. pMXs-FLAG- or Myc-LMIR4-IP and pMXs-FcRγ-IRES-blasticidin (pMXs-FcRγ-IB) were generated as described (2–4). To generate LMIR7 mutants (LMIR7-M1, -M2, and -M3) or LMIR4 mutants (LMIR4-M1 and -M2), two-step PCR mutagenesis (2–4) was performed by using pMXs-FLAG-LMIR7-IP or pMXs-FLAG-LMIR4-IP, respectively, as a template. LMIR7-M1 is the LMIR7(S189Y,V197E,V198L) mutant; LMIR7-M2 is the LMIR7(^{177}NSLFIW^{182}SRPHTR) mutant where six amino acid residues (NSLFIW) of LMIR7 were replaced with six amino acid residues (SRPHTR) of LMIR4 in the extracellular juxtamembrane region; LMIR7-M3 is the LMIR7(^{177}NSLFIW^{182}SRPHTR,S189Y,V197E,V198L) mutant; LMIR4-M1 is the LMIR4(Y177S,E185V,L186V) mutant; and LMIR4-M2 is the LMIR4(^{165}SRPHTR^{170}NSLFIW) mutant where six amino acid residues (SRPHTR) of LMIR4 were replaced with six amino acid residues (NSLFIW) of LMIR7 in the extracellular juxtamembrane region. All constructs were verified by DNA sequencing.

Transfection and Infection—Retroviral transfection was as described (1–4, 33, 34). Briefly, retroviruses were generated by transient transfection of PLAT-E packaging cells (34) with FuGENE 6 (Roche Diagnostics). Cells were infected with retroviruses in the presence of 10 μg/ml Polybrene. Selection with puromycin or blasticidin was started 48 h after infection.

Biochemistry—BMMCs expressing FLAG-tagged LMIR7 or mock were stimulated by 10 μg/ml anti-FLAG mAb or mouse IgG_1 mAb as control, 50 ng/ml SCF, or 10 μg/ml SPE-7 IgE for the indicated time as described (2–4, 28). To detect phosphorylation of several proteins, stimulated cells were lysed with Nonidet P-40 lysis buffer containing protease and phosphatase

inhibitor mixture (Sigma-Aldrich). To detect the interaction of LMIR7 and FcRγ, 293T cells were co-transfected with two constructs of interest. Cells were lysed with digitonin lysis buffer containing protease and phosphatase inhibitor mixture. Immunoprecipitation and Western blotting were done as described (1–4).

Flow Cytometry—Flow cytometric analysis of the stained cells was performed with a FACSCalibur (BD Biosciences) equipped with CellQuest software and Flowjo software (Tree Star) as described (2–4). Anti-LMIR7 mAb or rat IgG_1 mAb as control was biotinylated by sulfo-NHS-LC-biotin (Pierce) according to the manufacturer's instructions. Cells were incubated with 20 μg/ml biotin-anti-LMIR7 mAb or biotin-anti-rat IgG_1 mAb before incubation with PE-conjugated streptavidin. The geometric mean fluorescence intensity of Myc-tagged LMIR4, LMIR7, or its mutants was measured to evaluate its surface expression levels.

Measurement of Cytokines and Chemokines—For efficient stimulation of BMMC or FLMC, anti-biotin MACSiBead particles (Miltenyi Biotec) were used. Briefly, we prepared equal numbers of anti-biotin MACSiBead particles loaded with equal amounts of biotinylated anti-FLAG Ab, mouse IgG_1 mAb, anti-LMIR7 mAb, or rat IgG_1 mAb according to the manufacturer's instructions. Cells were stimulated by adding 2×10^6 anti-biotin MACSiBead particles to 1.5×10^5 cells in the presence or absence of 100 ng/ml lipopolysaccharide (LPS). After 24 h of stimulation, the concentrations of cytokines/chemokines in the supernatants were measured using enzyme-linked immunosorbent (ELISA) kits of IL-6, TNF-α, or MCP-1 from R&D Systems (2–4).

Statistical Analysis—Data are shown as the mean ± S.D., and statistical significance was determined by Student's *t* test with $p < 0.05$ taken as statistically significant.

RESULTS

Structure of LMIR7 in Comparison with LMIR4—We originally cloned LMIR1 using a signal sequence trap based on a retrovirus-mediated signal sequence trap (1, 35). LMIR2, -3, -4, and -5 were cloned by searching the GenBank™/EBI/DDBJ data bank using the sequence of the Ig-like domain of LMIR1 (1–3). Similarly, LMIR7 was cloned and identified from a BMMC cDNA library. LMIR7 protein from C57BL/6 mice is 245 amino acids in length. Like LMIR2, -4, and -5, LMIR7 is a type I transmembrane protein composed of an N-terminal signal peptide, an extracellular domain containing a single V-type Ig domain, a transmembrane domain, and a short cytoplasmic tail without any signaling motif. However, unlike typical activating receptors such as LMIR2 and LMIR5 (1–3), LMIR7 does not possess a positively charged residue in the transmembrane domain. An Ig-like domain of LMIR7 shares 85% identity at amino acid sequences with that of an inhibitory receptor, LMIR3/CLM-1, or an activating receptor, LMIR4/CLM-5 (Fig. 1*A*). In addition, LMIR7 differs from LMIR4 by only three amino acids in the transmembrane domain (Fig. 6*A*). The structural resemblance of LMIR7 to LMIR4 led us to analyze LMIR7 in comparison with LMIR4. First, we generated Ba/F3 cells expressing FLAG-tagged LMIR7, LMIR3, or LMIR4. Flow cytometric analysis using anti-FLAG mAb confirmed surface

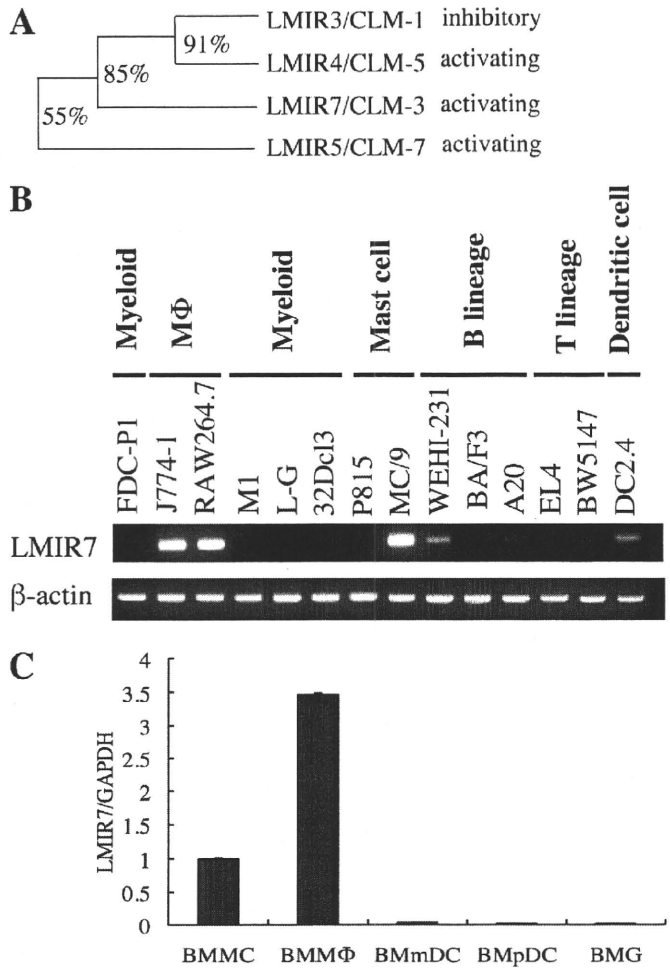

FIGURE 1. **LMIR7 expression at transcript levels in hematopoietic cells.** *A*, the phylogenetic tree of LMIR3/4/5/7 is shown based on homology with the Ig-like domain. The percentage of identity in amino acid sequences of the Ig-like domain was indicated. *B*, RT-PCR analysis on LMIR7 expression in murine hematopoietic cell lines. *C*, relative expression levels of LMIR7 among BMMC, BMMΦ, BMmDC, BMpDC, and BM granulocytes (*BMG*) were estimated by real-time PCR. The amount of expression was indicated relative to that in BMMC. Data are representative of three independent experiments.

expression of the transduced LMIR7 as well as LMIR3 and -4 (Fig. 2*A*). In addition, Western blot analysis demonstrated that similar to LMIR4, LMIR7 was detected by anti-FLAG mAb as two discrete bands (of 37 and 26 kDa) irrespective of reducing or nonreducing conditions (Fig. 2*B* and data not shown). Notably, LMIR7 were expressed more efficiently than LMIR4 at both surface expression and total protein levels (Fig. 2, *A* and *B*). Because LMIR7 protein possesses no apparent *N*-linked glycosylation sites but several *O*-glycosylation sites within its extracellular domain, we speculated that a band (37 kDa) corresponds to an *O*-glycosylated form of LMIR7 expressed on the cell surface. In accordance with this, *N*-glycosidase F treatment did not affect the mobility of LMIR7 (data not shown).

LMIR7 Is Highly Expressed in Mast Cells and Moncytes/Macrophages—To investigate the expression profile of LMIR7 in hematopoietic cells, we performed RT-PCR in a variety of hematopoietic cell lines. As a result, high expression levels of LMIR7 were observed in macrophage cell lines J774-1 and RAW264.7 and mast cell line MC/9 (Fig. 1*B*). In addition, we found detectable expression of LMIR7 in B-lineage cell lines

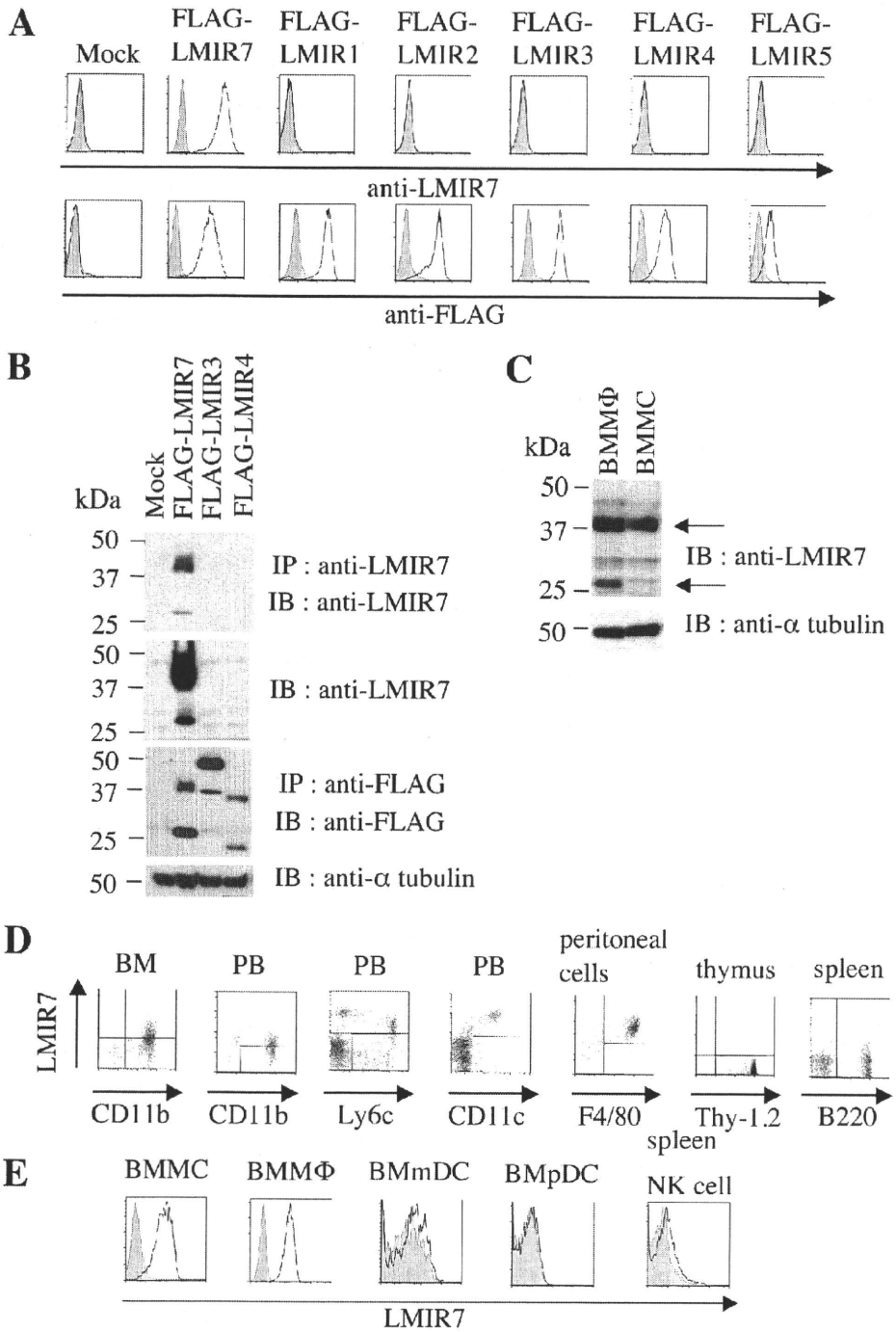

FIGURE 2. **Cell surface expression of LMIR7 in hematopoietic cells.** *A* and *B*, the sensitivity and specificity of anti-LMIR7 mAb were confirmed by flow cytometry (*A*) and Western blot (*B*). *A*, Ba/F3 cells were transduced with FLAG-tagged LMIR1, -2, -3, -4, -5, -7, or mock. The cells were stained with rat anti-LMIR7 mAb (*upper panel*) or mouse anti-FLAG mAb (*lower panel*) followed by PE-conjugated anti-rat IgG_1 Ab or anti-mouse IgG_1 Ab, respectively. *B*, lysates of Ba/F3 cells expressing FLAG-tagged LMIR3, -4, -7, or mock were immunoprecipitated with anti-LMIR7 mAb or rabbit anti-FLAG Ab and then immunoblotted with anti-LMIR7 mAb (*top panel*) or mouse anti-FLAG mAb (*third panel*), respectively. Total cell lysates were also immunoblotted with anti-LMIR7 mAb (*second panel*) or anti-α-tubulin Ab (*bottom panel*). *IB* and *IP* indicate immunoblot and immunoprecipitation, respectively. *C*, total cell lysates of BMMΦ or BMMC were immunoblotted with anti-LMIR7 mAb (*upper panel*) or anti-α-tubulin Ab (*lower panel*). *D*, analysis of LMIR7 expression in hematopoietic cells derived from C57 BL/6 mice. Single cell suspensions were prepared from BM, PB, peritoneal cavity, thymus, and spleen. Cells were stained with biotin anti-LMIR7 mAb or biotin rat IgG_1 mAb followed by PE-conjugated streptavidin and FITC-conjugated Abs as indicated. $FSC^{high}SSC^{high}$ populations in granulocytes or macrophages, $FSC^{low/int}SSC^{low/int}$ populations in lymphocytes cells, NK cells, or DC, or $FSC^{int}SSC^{int}$ populations in monocytes were gated and analyzed for LMIR7 expression. *E*, BMMC, BMMΦ, BMmDC, BMpDC, or $NK1.1^+$ spleen cells were stained with biotin anti-LMIR7 mAb or biotin rat IgG_1 mAb followed by PE-conjugated streptavidin. The result of control or LMIR7 staining is shown as a *filled* or *bold line histogram*, respectively. $NK1.1^+$ cells were sorted from spleen cells by using FITC-conjugated anti-NK1.1 Ab.

WEHI-231 and A20 and in a DC line, DC2.4, but not in other myeloid cell lines or T-lineage cell lines (Fig. 1*B*). On the other hand, real-time PCR analysis using BM-derived cells showed that expression levels of LMIR7 transcripts were specifically higher in BMMC and BMMΦ compared with BMmDC, BMpDC, or BM granulocytes (Fig. 1*C*, *BMG*). To examine the expression profiles of LMIR7 at protein levels, next we generated anti-LMIR7 mAb. As depicted in Fig. 2*A*, anti-LMIR7 mAb efficiently detected LMIR7 expressed on the surface of Ba/F3 cells transduced with FLAG-tagged LMIR7. This Ab did not detect any LMIR1, LMIR2, LMIR3, LMIR4, or LMIR5 transduced into Ba/F3 cells (Fig. 2*A*). These results verified the sensitivity and specificity of anti-LMIR7 mAb. Moreover, similar to anti-FLAG mAb, anti-LMIR7 mAb detected only FLAG-tagged LMIR7 alone, but not LMIR3 and LMIR4, as two discrete bands in the lysates of transduced Ba/F3 cells (Fig. 2*B*). However, unlike anti-FLAG Ab, anti-LMIR7 mAb more strongly detected a band with high molecular mass (37 kDa) compared with another band (23 kDa) (Fig. 2*B*), suggesting that anti-LMIR7 mAb reacted preferentially with the glycosylated form of LMIR7 expressed on the cell surface. We then stained hematopoietic cells using anti-LMIR7 mAb. Flow cytometric analysis demonstrated that LMIR7 was not expressed in B cells ($B220^+$) in BM or spleen, in T-lineage cells ($Thy\text{-}1.2^+$ or $CD3^+$) in PB, spleen, or thymus, or in NK cells ($NK1.1^+$) in spleen (Fig. 2, *D* and *E*, and data not shown). On the other hand, immature to mature neutrophils ($CD11b^{high}$) in BM or mature neutrophils ($CD11b^{high}$) in PB were $LMIR7^{dull/low}$, and monocytes ($Ly6c^{high}$) in PB were $LMIR7^{high}$ (Fig. 2*D*). Interestingly, a population of $CD11c^+$ cells in PB, but not in spleen, were $LMIR7^{high}$ (Fig. 2*D* and data not shown). Notably, peritoneal macrophages ($F4/80^+$) displayed high expression levels of

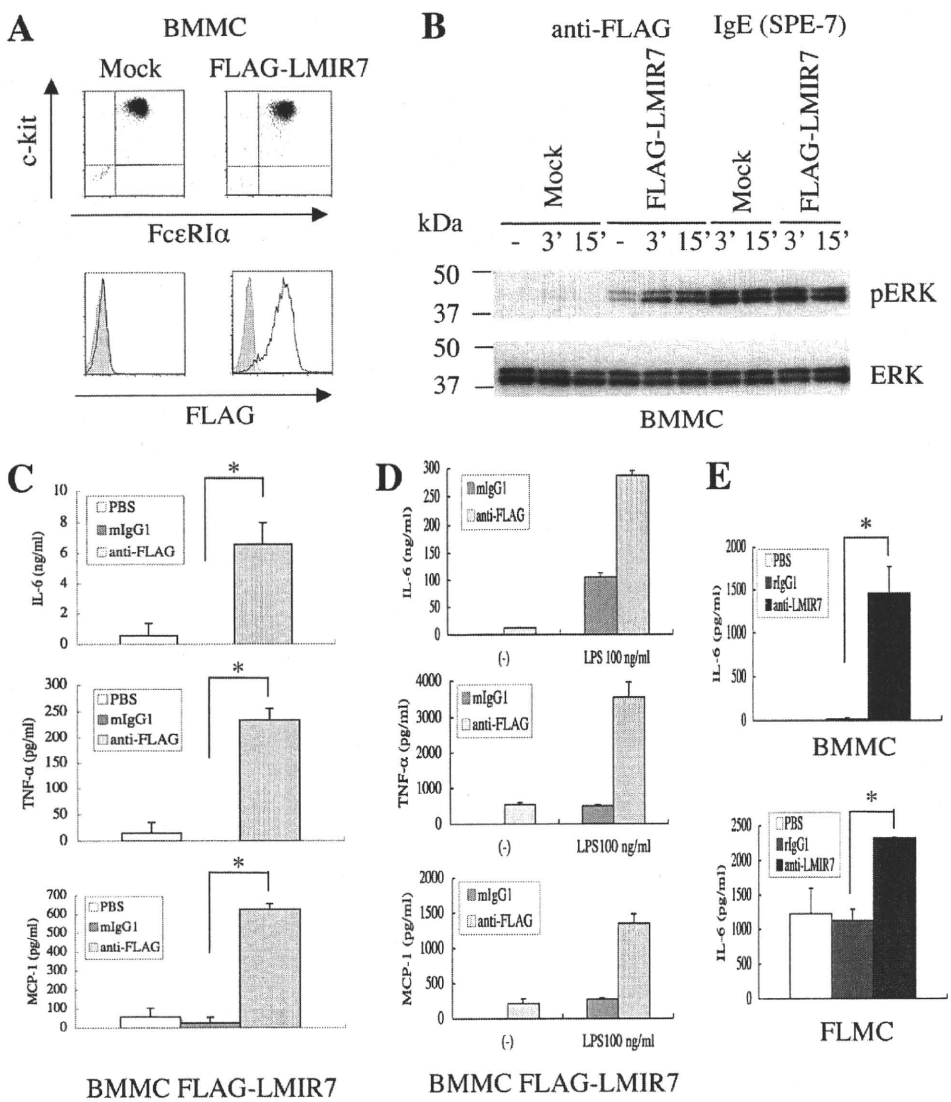

FIGURE 3. **Cross-linking of LMIR7 induced the phosphorylation of ERK in mast cells, resulting in cytokine/chemokine production.** *A*, the surface expression levels of c-Kit and FcεRIα in BMMC expressing FLAG-tagged LMIR7 or mock were analyzed by flow cytometry (*upper panel*). Cells were stained with FITC-conjugated anti-FLAG mAb (*lower panel*) as described. *B*, BMMC expressing FLAG-tagged LMIR7 or mock were stimulated with 10 μg/ml anti-FLAG mAb or 10 μg/ml IgE for 3 or 15 min as indicated. Cell lysates were subject to immunoblotting with anti-phospho-p44/42 MAPK (pERK1/2) Ab. The immunoblots were reprobed with Ab specific for ERK1/2. *C–E*, IL-6, TNF-α, and MCP-1 released into the culture supernatants were measured by ELISA. All data points correspond to the mean ± S.D. of three independent experiments. Statistically significant differences are shown. *, $p < 0.05$. *C*, BMMC expressing FLAG-tagged LMIR7 or mock were stimulated with anti-FLAG Ab, mouse IgG_1, or PBS for 24 h as described under "Experimental Procedures." *D*, BMMC expressing FLAG-tagged LMIR7 or mock were stimulated with anti-FLAG Ab or mouse IgG_1 in the presence or absence of 100 ng/ml LPS as described under "Experimental Procedures." *E*, BMMC (*upper panel*) or FLMC (*lower panel*) were stimulated with anti-LMIR7 mAb or rat IgG_1 for 24 h as described under "Experimental Procedures."

LMIR7 (Fig. 2*D*). When BMMC, BMmDC, BMpDC, and BMMΦ were stained with anti-LMIR7 mAb, we found that BMmDC and BMpDC expressed scarcely detectable levels of LMIR7 (Fig. 2*E*). Remarkably, LMIR7 was expressed at high levels in BMMC as well as in BMMΦ (Fig. 2*E*). Taken together with the results on LMIR7 expression at transcript levels, these findings indicated that LMIR7 was not expressed in lymphoid-lineage cells, except for a few B-lineage cell lines, but was broadly expressed in myeloid-lineage cells. Importantly, LMIR7 was highly expressed in mast cells, monocytes/macrophages, and a small subset of $CD11c^+$ cells in PB. High expression levels of endogenous LMIR7 in BMMC and BMMΦ were also confirmed by Western blot analysis (Fig. 2*C*). Because LMIR4 is predominantly expressed in neutrophils, the present results indicated that LMIR7 and LMIR4 were differentially distributed in hematopoietic cells.

LMIR7 Engagement Induced the Activation of BMMC—In view of expression profiles of LMIR7, we examined the functions of LMIR7 in mast cells. BMMCs were retrovirally transduced with either FLAG-tagged LMIR7 or mock. We found comparable expression levels of c-Kit and FcεRI in both BMMCs and confirmed the expression of transduced LMIR7 by staining with anti-FLAG mAb (Fig. 3*A*). In addition, transduction with LMIR7 did not affect the differentiation or the growth of BMMCs (data not shown). Although stimulation with IgE induced equivalent levels of ERK phosphorylation in both BMMCs, stimulation with anti-FLAG mAb led to ERK activation only in LMIR7-transduced BMMCs (Fig. 3*B*). Accordingly, stimulation with anti-FLAG mAb-loaded beads resulted in robust cytokine/chemokine (IL-6, TNF-α, and MCP-1) production of BMMCs expressing FLAG-LMIR7 (Fig. 3*C*). We confirmed that stimulation with control Ab-coated beads did not induce significant levels of cytokine/chemokine production in these cells (Fig. 3*C*). On the other hand, a similar stimulation did not cause degranulation, characterized by β-hexosaminidase release, of the LMIR7-transduced BMMCs (data not shown). Interestingly, cross-linking of LMIR7 synergistically enhanced the cytokine/chemokine production of LMIR7-transduced BMMC stimulated by LPS through TLR4 (Fig. 3*D*). Importantly, BMMC or FLMC produced significant levels of IL-6 when endogenous LMIR7 was engaged with anti-LMIR7 mAb-loaded beads but not control Ab-loaded beads (Fig. 3*E*). Collectively, our results show that LMIR7 cross-linking alone induced the activation of mast cells leading to cytokine/chemokine production, demonstrating that LMIR7 is an activating receptor.

FcRγ Deficiency Did Not Affect Surface Expression Levels of LMIR7 in Mast Cells or Macrophages but Dampened Cytokine Production of Mast Cells Stimulated by LMIR7 Cross-linking—LMIR4 transmits an activating signal by interacting with FcRγ

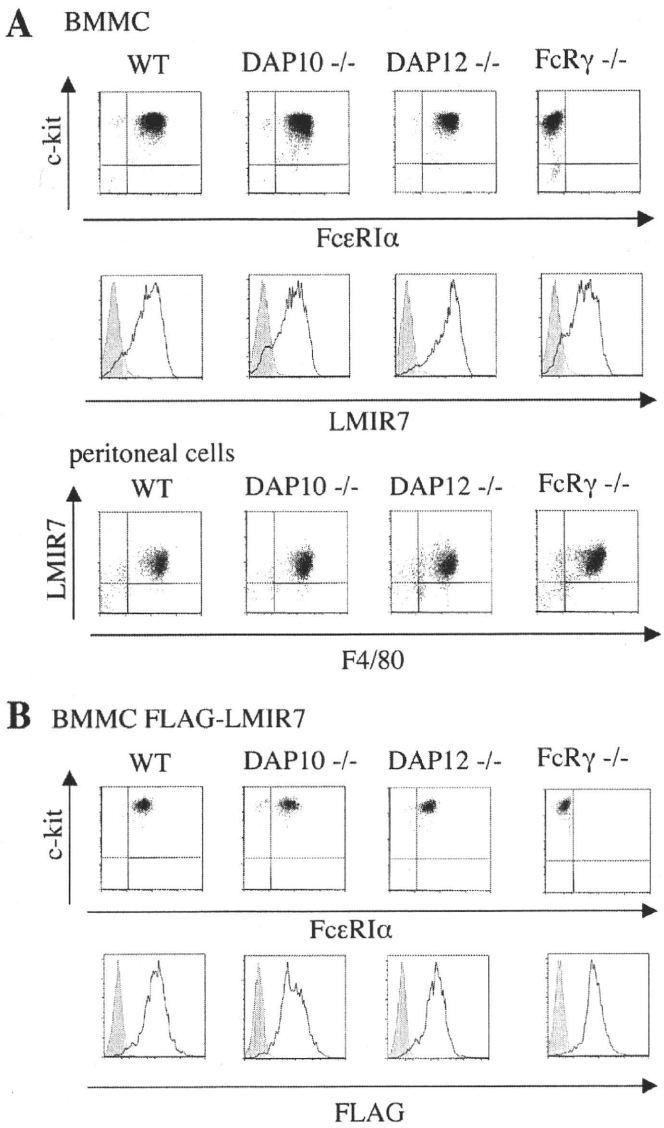

FIGURE 4. **FcRγ is dispensable for surface expression in mast cells or macrophages.** *A*, surface expression levels of endogenous LMIR7 (*middle panel*) or c-Kit and FcεRIα (*top panel*) in BMMC derived from WT, *DAP10*$^{-/-}$, *DAP12*$^{-/-}$, or *FcRγ*$^{-/-}$ mice were analyzed as described in the legend for Fig. 3*A*. Surface expression levels of endogenous LMIR7 and F4/80 (*bottom panel*) in peritoneal cells derived from WT, *DAP10*$^{-/-}$, *DAP12*$^{-/-}$, or *FcRγ*$^{-/-}$ mice were analyzed as described in the legend for Fig. 2*D*. *B*, surface expression levels of FLAG-tagged LMIR7 (*lower panel*) or c-Kit and FcεRIα (*upper panel*) in FLAG-tagged LMIR7-transduced BMMC derived from WT, *DAP10*$^{-/-}$, *DAP12*$^{-/-}$, or *FcRγ*$^{-/-}$ mice were analyzed as described.

among adaptor molecules containing ITAM or the related activating motif-bearing molecules (2). We asked which adaptor molecule plays an important role in LMIR7-mediated activating signal. Flow cytometric analysis demonstrated that surface expression levels of LMIR7 did not differ among wild type (WT) and DAP10, DAP12, or FcRγ-deficient peritoneal MΦ or BMMC (Fig. 4*A*). We confirmed that surface expression levels of FcεRI and c-Kit among these BMMCs were comparable and that those of FcεRI in FcRγ-deficient BMMC were not detectable (Fig. 4*A*), as reported (2, 16). In addition, neither DAP10/DAP12 nor DAP12/FcRγ double deficiency affected surface expression levels of LMIR7 (data not shown). Moreover, when LMIR7 was transduced into DAP10-, DAP12-, or FcRγ-deficient or WT BMMC, the surface expression levels of transduced LMIR7 as well as FcεRI and c-Kit were comparable among these transfectants (Fig. 4*B*). We confirmed that FcεRI expression was not detectable in FcRγ-deficient BMMC (Fig. 4*B*) as reported (16). Taken together, these results indicated that DAP10, DAP12, or FcRγ did not affect surface expression levels of LMIR7. To examine whether adaptor molecules are involved in LMIR7 functions, we stimulated these transfectants with anti-FLAG mAb- or control mAb-loaded beads. Strikingly, LMIR7-mediated cytokine production was abolished by a deficiency in FcRγ but not DAP10 or DAP12, although we found comparable levels of cytokine production among these cells stimulated using phorbol 12-myristate 13-acetate as control (Fig. 5*A*). Consistently, ERK activation of LMIR7-transduced BMMC stimulated by LMIR7 cross-linking, but not by SCF as control, was absent in FcRγ-deficient cells (Fig. 5*B*). We then asked whether LMIR7 physically associated with FcRγ. To this end, 293T cells were co-transfected with FcRγ or a control construct together with a FLAG-tagged LMIR7 or a control construct. Co-immunoprecipitation experiments demonstrated that FcRγ interacted significantly with LMIR7 (Fig. 5*C*). Collectively, these results indicated that FcRγ was required for LMIR7-mediated activation signaling but was dispensable for surface expression of LMIR7.

Strong Interaction of LMIR4 with FcRγ in Comparison with LMIR7 Depended on the Extracellular Juxtamembrane Region and the Transmembrane Domain of LMIR4—In the course of this study, we found that FcRγ were less efficiently co-immunoprecipitated with LMIR7 in comparison with LMIR4 (Fig. 6*C* and data not shown). We next sought to dermine the molecular mechanism by which LMIR4-FcRγ interaction becomes stronger than LMIR7-FcRγ interaction. As shown in Fig. 6*A*, LMIR7 differed from LMIR4 by only three amino acid residues in the transmembrane domain. As it is generally accepted that a transmembrane structure plays a critical role in receptor interaction (15, 24, 25), we generated a chimera receptor composed of an extracellular domain, LMIR7, a transmembrane domain, LMIR4, and an intracellular domain, LMIR7, designated LMIR7-M1. When Ba/F3 cells were transduced with Myc-tagged LMIR-M1 as well as Myc-tagged LMIR4, LMIR7, or mock, flow cytometric analysis using anti-Myc mAb showed that surface expression levels of LMIR7-M1 were equivalent to those of LMIR4 and lower than those of LMIR7 (Fig. 6*B*). These results indicated that the transmembrane domain of LMIR7 was indispensable for maintaining surface expression of LMIR7 at high levels. Interestingly, further transduction with FcRγ into these Ba/F3 cells weakly or moderately increased the surface expression levels of LMIR7-M1 or LMIR4, respectively, although it did not affect those of LMIR7 (Fig. 6*B*). We also performed co-immunoprecipitation experiments similar to those described in Fig. 5*C*. Notably, FcRγ was efficiently co-immunoprecipitated with LMIR7-M1 in comparison with LMIR7, whereas the amount of FcRγ co-immunoprecipitated with LMIR7-M1 was still lower than that co-immunoprecipitated with LMIR4 (Fig. 6*C*). These results led us to ask whether a structural domain other than the transmembrane domain of LMIR4 was involved in the tight interaction between LMIR4 and

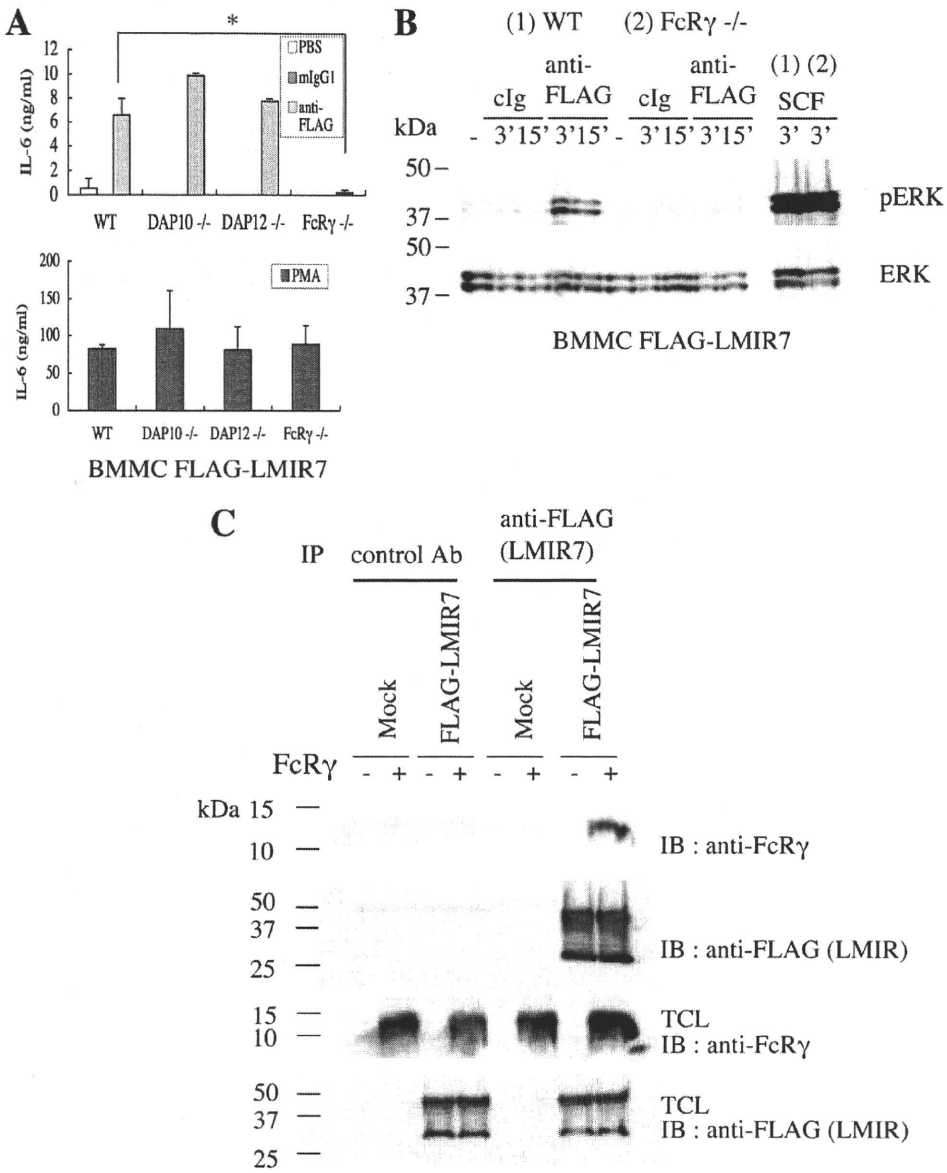

FIGURE 5. **FcRγ is required for LMIR7-mediated activation of mast cells.** *A*, IL-6 released into the culture supernatants was measured by ELISA. WT, *DAP10*$^{-/-}$, *DAP12*$^{-/-}$, or *FcRγ*$^{-/-}$ BMMC expressing FLAG-tagged LMIR7 were stimulated with anti-FLAG mAb, mouse IgG_1, or PBS (*upper panel*) or 50 nM phorbol 12-myristate 13-acetate (*PMA*, *lower panel*) for 24 h as described under "Experimental Procedures." All data points correspond to the mean ± S.D. of three independent experiments. Statistically significant differences are shown. *, $p < 0.05$. *B*, WT or *FcRγ*$^{-/-}$ BMMC expressing FLAG-tagged LMIR7 were stimulated with 10 μg/ml anti-FLAG Ab or mouse IgG_1 or 50 ng/ml SCF for the indicated time. Cell lysates were subject to immunoblotting with anti-phospho-p44/42 MAPK (pERK1/2) Ab. The immunoblots were reprobed with Ab specific for ERK1/2. *C*, 293T cells were transiently co-transfected with a FLAG-tagged LMIR7 or mock and an FcRγ construct or mock. Immunoprecipitates of lysates of these transfectants with anti-FLAG mAb were probed with polyclonal anti-FcRγ Ab or anti-FLAG mAb. One representative of three independent experiments is shown. *IB* and *IP* indicate immunoblot and immunoprecipitation, respectively. *TCL* indicates total cell lysates.

FcRγ. We paid attention to the difference of six amino acid residues (SRPHTR *versus* NSLFIW) in the extracellular juxtamembrane domain of LMIR4 *versus* LMIR7 (Fig. 6*A*). We additionally generated two types of chimera receptors: LMIR7-M2, where an extracellular juxtamembrane region of LMIR7 was replaced with that of LMIR4, and LMIR7-M3, where both an extracellular juxtamembrane region and a transmembrane domain were replaced with those of LMIR4 (Fig. 6*A*). Myc-tagged LMIR7-M2 or LMIR7-M3 was transduced into Ba/F3 cells, demonstrating that surface expression levels of LMIR7-M2 were higher than those of LMIR7 and that surface expression levels of LMIR7-M3 were lower and higher than those of LMIR-M2 and LMIR-M1, respectively (Fig. 6*B*). On the other hand, the presence of FcRγ weakly or moderately increased the surface expression levels of LMIR7-M2 or LMIR7-M3, respectively (Fig. 6*B*). Intriguingly, the amount of FcRγ co-immunoprecipitated with LMIR7-M2 or LMIR7-M3 was comparable with that co-immunoprecipitated with LMIR7-M1 or LMIR4, respectively (Fig. 6*C*). Collectively, these results indicated that the extracellular juxtamembrane region of LMIR4 had a positive effect on its surface expression levels, whereas the transmembrane domain of LMIR4 had a negative effect. In addition, the extracellular juxtamembrane region as well as the transmembrane domain of LMIR4 played a critical role in the strong interaction between LMIR4 and FcRγ. For further analysis, we generated two chimeric receptors: LMIR4-M1, where the transmembrane domain of LMIR4 was replaced with that of LMIR7, and LMIR4-M2, where the extracellular juxtamembrane region was replaced with that of LMIR7 (Fig. 6*A*). Myc-tagged LMIR4-M1 or LMIR4-M2 was transduced into Ba/F3 cells, demonstrating that surface expression levels of LMIR4-M1 or LMIR4-M2 were higher or lower, respectively, than those of LMIR4 (Fig. 6*D*). These results indicated the negative effect of the extracellular juxtamembrane region of LMIR7 on its surface expression levels, as well as the positive effect of the transmembrane domain of LMIR7. The presence of FcRγ did not significantly increase the surface expression levels of LMIR4-M1 or LMIR4-M2 (Fig. 6*D*). We found that FcRγ co-immunoprecipitated with LMIR4-M1 or LMIR4-M2, but the amount of FcRγ co-immunoprecipitated with LMIR4-M1 or LMIR4-M2 was lower than that co-immunoprecipitated with LMIR4 (Fig. 6*E*). It should be noted that the amount of FcRγ co-immunoprecipitated with LMIR4-M1 was lower than that co-immunoprecipitated with LMIR4-M2, notwithstanding the higher expression levels of LMIR4-M1 in comparison with LMIR4-M2 (Fig. 6*E*). Taken together, these results suggested that both the transmembrane domain and the extracellular juxtamembrane

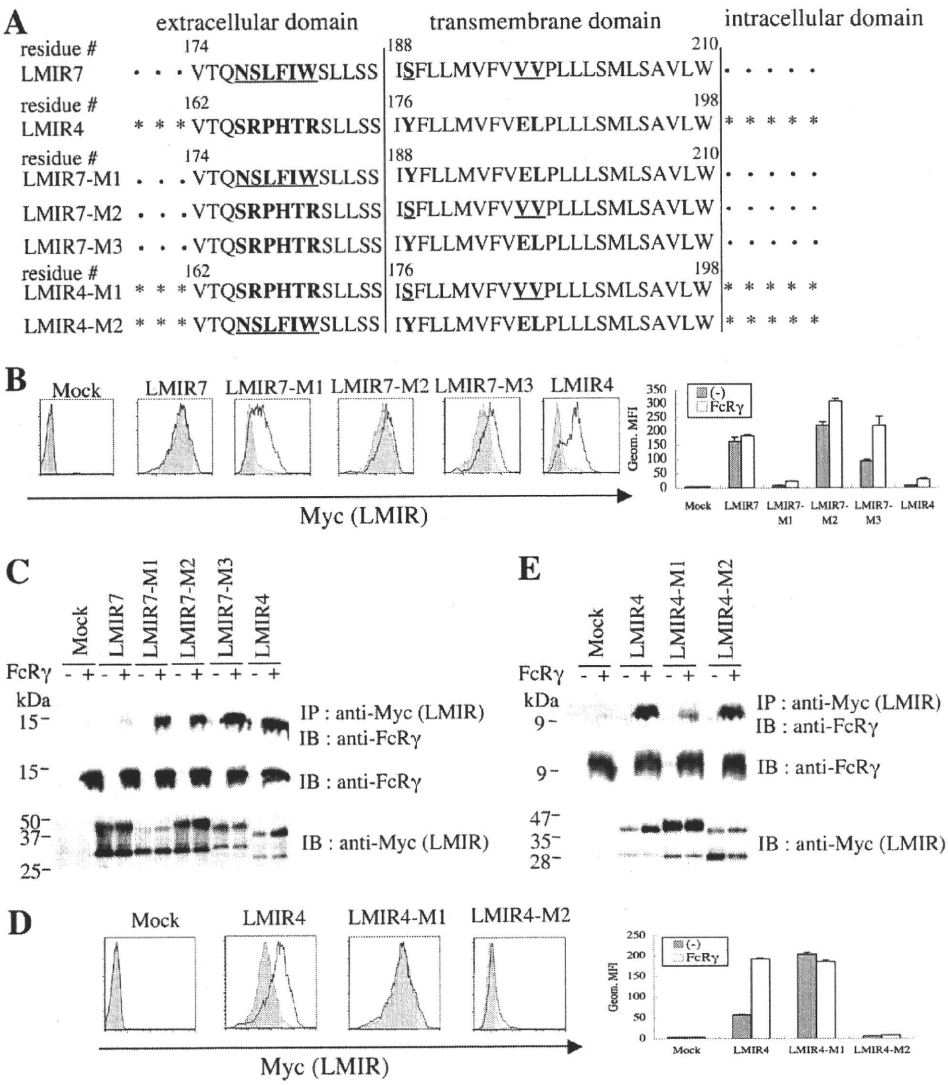

FIGURE 6. **Both the extracellular juxtamembrane region and the transmembrane domain of LMIR4 are indispensable for stronger association of LMIR4-FcRγ as compared with LMIR7-FcRγ.** *A*, alignment of amino acid sequences of the extracellular juxtamembrane and transmembrane domains in LMIR4, LMIR7, and chimera receptors (LMIR7-M1, LMIR7-M2, LMIR7-M3, LMIR4-M1, and LMIR4-M2) are shown using SMART (simple modular architecture research tool) software. Different amino acid residues between LMIR4/CLM-5 (GenBank™ accession number AY457051) and LMIR7/CLM-3 (GenBank™ accession number AY457049) in extracellular juxtamembrane and transmembrane domains are shown in *boldface*, and among these LMIR7-specific amino acid residues are *underlined*. A dot (·) or an asterisk (*) indicates an amino acid residue of the extracellular and intracellular domains of LMIR7 or LMIR4, respectively. *B*, Ba/F3 cells were transduced with (Myc-tagged LMIR7, LMIR7-M1, LMIR7-M2, LMIR7-M3, LMIR4, or mock) plus (FcRγ or alone). Cells were stained with FITC-conjugated anti-Myc mAb. The results of staining (*left panel*) are shown as a *filled histogram* (Ba/F3 cells without FcRγ) or *bold line histogram* (Ba/F3 cells expressing FcRγ). The geometric mean fluorescence intensities (*Geom. MFI*) of Myc-tagged receptors were measured by flow cytometry (*right panel*). All data points correspond to the mean ± S.D. of three independent experiments. One representative of three independent experiments is shown. *C*, 293T cells were transiently co-transfected with (a Myc-tagged LMIR7, LMIR7-M1, LMIR7-M2, LMIR7-M3, LMIR4, or mock) and (an FcRγ construct or alone). Immunoprecipitates of the lysates of these transfectants with anti-Myc mAb were probed with anti-FcRγ Ab. Total cell lysates of these transfectants were also immunoblotted with anti-FcRγ Ab or anti-Myc mAb. One representative of three independent experiments is shown. *IB* and *IP* indicate immunoblot and immunoprecipitation, respectively. *D*, Ba/F3 cells were transduced with (Myc-tagged LMIR4, LMIR4-M1, LMIR4-M2, or mock) plus (FcRγ or mock). Cells were stained with anti-Myc mAb or mouse IgG_1 as control followed by PE-conjugated anti-mouse IgG goat $F(ab')_2$ Ab. The results of staining (*left panel*) are shown as a *filled histogram* (Ba/F3 cells without FcRγ) or *bold line histogram* (Ba/F3 cells expressing FcRγ). The geometric mean fluorescence intensities of Myc-tagged receptors were measured by flow cytometry (*right panel*). All data points correspond to the mean ± S.D. of three independent experiments. One representative of three independent experiments is shown. *E*, 293T cells were transiently co-transfected with (a Myc-tagged LMIR4, LMIR4-M1, LMIR4-M2, or mock) and (an FcRγ construct or alone). Immunoprecipitates of lysates of these transfectants with anti-Myc mAb were probed with anti-FcRγ Ab. Total cell lysates of these transfectants were also immunoblotted with anti-FcRγ Ab or anti-Myc mAb. One representative of three independent experiments is shown.

region of LMIR4 were required, but in different ways, for the efficient up-regulation of surface LMIR4 by the LMIR4-FcRγ interaction.

DISCUSSION

In the present study, we have characterized LMIR7 as an activating receptor closely related to LMIR4 among the LMIR family receptors. Homology research has indicated that LMIR7 is similar to LMIR4 in structure: between them, 85% of the Ig-like domain and 87% of the transmembrane domain are identical in amino acid sequences. Interestingly, neither LMIR7 nor LMIR4 possesses a positively charged residue in the transmembrane domain that is thought to be required for the interaction with ITAM or related activating motif-bearing adaptor proteins. However, our conclusion that, like LMIR4, LMIR7 interacts with FcRγ and thereby transmits an activating signal is based on the following findings: cross-linking of LMIR7 induces ERK activation and cytokine production in BMMC; these activation events are dampened by FcRγ deficiency; and FcRγ is co-immunoprecipitated with LMIR7.

Notably, despite the high homology of the transmembrane domains, several differences exist between LMIR7 and LMIR4. LMIR7-FcRγ interaction is weaker than LMIR4-FcRγ interaction; surface expression levels of LMIR7 are higher than those of LMIR4 (Fig. 6). Our analysis of chimera receptors delineated the relevant molecular mechanism. The transmembrane domain of LMIR7 played a role in maintaining its surface expression at high levels, and probably no charged residue in the transmembrane domain stabilized LMIR7 on the cell surface even in the absence of FcRγ. Interestingly, the extracellular juxtamembrane region of LMIR7 had a negative effect on its surface expression levels, whereas that of LMIR4 had a positive effect. We also reasoned that FcRγ expression did not further increase the surface expression of LMIR7, presumably because of the

weak interaction of LMIR7 with FcRγ. In addition, the weak but significant levels of LMIR7-FcRγ interaction might be explained by a leucine zipper-like interaction between the transmembrane region of LMIR7 and FcRγ. As reported (25), a leucine zipper-like interaction formed by FcRγ residues (Leu-14 and Leu-21) and FcαRI residues (Leu-217, Leu-220, and Leu-224) as well as an Arg/Asp charge interaction formed by the FcRγ residue (Asp-11) and the FcαRI residue (Arg-209) contribute to the tight interaction of both receptors. Interestingly, both LMIR7 and LMIR4 maintain the leucine zipper-like sequences in the transmembrane: LMIR7 residues Leu-202, Leu-205, and Leu-209; and LMIR4 residues Leu-190, Leu-193, and Leu-197. Therefore, it is possible that the leucine zipper-like sequences in the transmembrane of LMIR7 play a role in the LMIR7-FcRγ interaction. In addition, the transmembrane domain of LMIR7 probably contributes to the LMIR7-FcRγ interaction by maintaining surface LMIR7 at high levels. Alternatively, an unknown adaptor molecule might intervene between LMIR7 and FcRγ. Further examination will be necessary to completely understand the precise mechanism of how LMIR7 interacts with FcRγ.

On the other hand, we also speculated that some other mechanism was involved in the strong interaction of LMIR4 with FcRγ. Indeed, we clearly demonstrated by analysis done on chimera receptors that the extracellular juxtamembrane region (amino acid sequence SPRHTR) of LMIR4 played a critical role in the up-regulation of surface LMIR4 by its interaction with FcRγ (Fig. 6). Because there is variability in terms of the expression levels of the chimeric or parent receptors, it is difficult to assess the relative importance of a transmembrane domain *versus* an extracellular juxtamembrane region. However, our results suggested that the transmembrane domain of LMIR4 plays a major role in the high affinity interaction of LMIR4 with FcRγ (Fig. 6*E*). Although the cytoplasmic region, as well as the transmembrane domain, of GPVI is reportedly required for its interaction with FcRγ (23), to our knowledge the present work is the first demonstration that an extracellular juxtamembrane region of an activating receptor plays an important part in the tight interaction with FcRγ. One possibility is that the extracellular juxtamembrane region of LMIR4 interacts with the short extracellular domain of FcRγ. Alternatively, the extracellular juxtamembrane region of LMIR4 might be folded in three-dimensional structure and thereby kept in contact with the transmembrane domain of FcRγ. According to a recent report (24), three polar positions formed by one basic T cell receptor (TCR) α and two ζζ basic aspartic acid transmembrane residues are critical for ζζ dimerization and assembly with T cell receptor. In most cases, this theory is probably valid for activating receptors coupled with FcRγ, considering the high degree of sequence homology between ζ and FcRγ. However, in FcRγ-coupled receptors without a positively charged residue in the transmembrane, the notion presented in this study highlights the novel molecular mechanism of the interaction between activating receptors and FcRγ.

Whereas LMIR4 is expressed predominantly in neutrophils (4), real-time PCR and flow cytometric analysis demonstrated that LMIR7 is highly expressed in mast cells and monocytes/macrophages. Notably, high expression levels of LMIR7 were also observed in an immature subtype of dendritic cell ($CD11c^+$) in PB but not in myeloid or plasmacytoid dendritic cells. Because an inhibitory LMIR3 is broadly expressed in myeloid cells (2, 4), it is likely that LMIR3 pairs with LMIR7 in mast cells and monocytes/macrophages or with LMIR4 in neutrophils. Intriguingly, we showed previously that LMIR3 transmits an inhibitory signal while it interacts with FcRγ and thereby transmits an activating signal in concert with an LPS/TLR4 signal (4). In addition, we demonstrated that like the LMIR4 signal, the LMIR7 signal synergizes with the LPS signal. Therefore, if LMIR3/4/7, with a highly conserved Ig-like domain, had a similar or the same ligand, the LMIR3 signal might inhibit the LMIR7-mediated activating signal or, conversely, cooperate with the LMIR7 signal to enhance the TLR4 signal *in vivo*. In any case, it is possible that LMIR7 or LMIR4 modulates the innate immune responses in a cell type-dependent manner. Complete understanding of the *in vivo* functions of LMIR requires both analysis of each of the knock-out mice and identification of the ligands of each LMIR.

In conclusion, LMIR7 is an activating receptor found among the LMIR family, which transmits an activating signal by interacting with FcRγ. LMIR7 shares similarities with LMIR4 as a counterpart of LMIR3, whereas LMIR7 is regulated differently from LMIR4 in regard to distribution, expression, and function, suggesting a nonredundant role for both activating receptors in other cell types.

Acknowledgments—We thank Dr. Hisashi Arase for providing the pME18S expression vector containing a mouse CD150 leader segment (32). We also thank Dr. Marco Colonna for providing DAP10$^{-/-}$ mice (30). We are grateful to Dr. Dovie Wylie for excellent language assistance.

REFERENCES

1. Kumagai, H., Oki, T., Tamitsu, K., Feng, S. Z., Ono, M., Nakajima, H., Bao, Y. C., Kawakami, Y., Nagayoshi, K., Copeland, N. G., Gilbert, D. J., Jenkins, N. A., Kawakami, T., and Kitamura, T. (2003) *Biochem. Biophys. Res. Commun.* **307,** 719–729
2. Izawa, K., Kitaura, J., Yamanishi, Y., Matsuoka, T., Oki, T., Shibata, F., Kumagai, H., Nakajima, H., Maeda-Yamamoto, M., Hauchins, J. P., Tybulewicz, V. L., Takai, T., and Kitamura, T. (2007) *J. Biol. Chem.* **282,** 17997–18008
3. Yamanishi, Y., Kitaura, J., Izawa, K., Matsuoka, T., Oki, T., Lu, Y., Shibata, F., Yamazaki, S., Kumagai, H., Nakajima, H., Maeda-Yamamoto, M., Tybulewicz, V. L., Takai, T., and Kitamura, T. (2008) *Blood* **111,** 688–698
4. Izawa, K., Kitaura, J., Yamanishi, Y., Matsuoka, T., Kaitani, A., Sugiuchi, M., Takahashi, M., Maehara, A., Enomoto, Y., Oki, T., Takai, T., and Kitamura, T. (2009) *J. Immunol.* **183,** 925–936
5. Chung, D. H., Humphrey, M. B., Nakamura, M. C., Ginzinger, D. G., Seaman, W. E., and Daws, M. R. (2003) *J. Immunol.* **171,** 6541–6548
6. Yotsumoto, K., Okoshi, Y., Shibuya, K., Yamazaki, S., Tahara-Hanaoka, S., Honda, S., Osawa, M., Kuroiwa, A., Matsuda, Y., Tenen, D. G., Iwama, A., Nakauchi, H., and Shibuya, A. (2003) *J. Exp. Med.* **198,** 223–233
7. Luo, K., Zhang, W., Sui, L., Li, N., Zhang, M., Ma, X., Zhang, L., and Cao, X. (2001) *Biochem. Biophys. Res. Commun.* **287,** 35–41
8. Fujimoto, M., Takatsu, H., and Ohno, H. (2006) *Int. Immunol.* **18,** 1499–1508
9. Daish, A., Starling, G. C., McKenzie, J. L., Nimmo, J. C., Jackson, D. G., and Hart, D. N. (1993) *Immunology* **79,** 55–63
10. Bachelet, I., Munitz, A., Moretta, A., Moretta, L., and Levi-Schaffer, F. (2005) *J. Immunol.* **175,** 7989–7995

11. Alvarez-Errico, D., Aguilar, H., Kitzig, F., Brckalo, T., Sayós, J., and López-Botet, M. (2004) *Eur. J. Immunol.* **34,** 3690–3701
12. Ravetch, J. V., and Lanier, L. L. (2000) *Science* **290,** 84–89
13. Takai, T., and Ono, M. (2001) *Immunol. Rev.* **181,** 215–222
14. Colonna, M. (2003) *Nat. Rev. Immunol.* **3,** 445–453
15. Humphrey, M. B., Lanier, L. L., and Nakamura, M. C. (2005) *Immunol. Rev.* **208,** 50–65
16. Takai, T., Li, M., Sylvestre, D., Clynes, R., and Ravetch, J. V. (1994) *Cell* **76,** 519–529
17. Blank, U., Ra, C., Miller, L., White, K., Metzger, H., and Kinet, J. P. (1989) *Nature* **337,** 187–189
18. Scholl, P. R., and Geha, R. S. (1993) *Proc. Natl. Acad. Sci. U.S.A.* **90,** 8847–8850
19. Ra, C., Jouvin, M. H., Blank, U., and Kinet, J. P. (1989) *Nature.* **341,** 752–754
20. Pfefferkorn, L. C., and Yeaman, G. R. (1994) *J. Immunol.* **153,** 3228–3236
21. Morton, H. C., van den Herik-Oudijk, I. E., Vossebeld, P., Snijders, A., Verhoeven, A. J., Capel, P. J., and van de Winkel, J. G. (1995) *J. Biol. Chem.* **270,** 29781–29787
22. Maeda, A., Kurosaki, M., and Kurosaki, T. (1998) *J. Exp. Med.* **188,** 991–995
23. Bori-Sanz, T., Inoue, K. S., Berndt, M. C., Watson, S. P., and Tulasne, D. (2003) *J. Biol. Chem.* **278,** 35914–35922
24. Call, M. E., Schnell, J. R., Xu, C., Lutz, R. A., Chou, J. J., and Wucherpfennig, K. W. (2006) *Cell* **127,** 355–368
25. Wines, B. D., Trist, H. M., Ramsland, P. A., and Hogarth, P. M. (2006) *J. Biol. Chem.* **281,** 17108–17113
26. Kawakami, T., and Galli, S. J. (2002) *Nat. Rev. Immunol.* **2,** 773–786
27. Kraft, S., and Kinet, J. P. (2007) *Nat. Rev. Immunol.* **7,** 365–378
28. Kitaura, J., Song, J., Tsai, M., Asai, K., Maeda-Yamamoto, M., Mocsai, A., Kawakami, Y., Liu, F. T., Lowell, C. A., Barisas, B. G., Galli, S. J., and Kawakami, T. (2003) *Proc. Natl. Acad. Sci. U.S.A.* **100,** 12911–12916
29. Kawakami, T., and Kitaura, J. (2005) *J. Immunol.* **175,** 4167–4173
30. Gilfillan, S., Ho, E. L., Cella, M., Yokoyama, W. M., and Colonna, M. (2002) *Nat. Immunol.* **3,** 1150–1155
31. Kaifu, T., Nakahara, J., Inui, M., Mishima, K., Momiyama, T., Kaji, M., Sugahara, A., Koito, H., Ujike-Asai, A., Nakamura, A., Kanazawa, K., Tan-Takeuchi, K., Iwasaki, K., Yokoyama, W. M., Kudo, A., Fujiwara, M., Asou, H., and Takai, T. (2003) *J. Clin. Invest.* **111,** 323–332
32. Shiratori, I., Ogasawara, K., Saito, T., Lanier, L. L., and Arase, H. (2004) *J. Exp. Med.* **199,** 525–533
33. Kitamura, T., Koshino, Y., Shibata, F., Oki, T., Nakajima, H., Nosaka, T., and Kumagai, H. (2003) *Exp. Hematol.* **31,** 1007–1014
34. Morita, S., Kojima, T., and Kitamura, T. (2000) *Gene Ther.* **7,** 1063–1066
35. Kojima, T., and Kitamura, T. (1999) *Nat. Biotechnol.* **17,** 487–490